



Optimization of the manufacturing process for sheet metal panels
considering shape, tessellation and structural stability

Optimierung des Herstellungsprozesses von dünnwandigen, profilierten
Aussenwandpaneelen

by

Fasih Mohiuddin Syed

from

Mysore, India

A Master thesis submitted to the Institute of Construction Informatics, Faculty of Civil
Engineering, University of Technology Dresden in partial fulfilment of the requirements for the
degree of

Master of Science

Responsible Professor : Prof. Dr.-Ing. habil. Karsten Menzel

Second Examiner : Prof. Dr.-Ing. Raimar Scherer

Advisor : Dipl.-Ing. Johannes Frank Schüler

Dresden, 14th April, 2020

Task Sheet

Declaration

I confirm that this assignment is my own work and that I have not sought or used the inadmissible help of third parties to produce this work. I have fully referenced and used inverted commas for all text directly quoted from a source. Any indirect quotations have been duly marked as such.

This work has not yet been submitted to another examination institution – neither in Germany nor outside Germany – neither in the same nor in a similar way and has not yet been published.

Dresden,

Place, Date

(Signature)

Acknowledgement

First, I would like to express my sincere gratitude to Prof. Dr.-Ing. habil. Karsten Menzel, Chair of the "Institute of Construction Informatics" for giving me this opportunity to work on my master thesis and believing in my work.

I am very grateful to Dipl.-Ing. Johannes Frank Schüler for his encouragement, guidance and support during the course of work. I would like to thank all the staff from "Institute of Construction Informatics " for their valuable support.

I must express my very profound gratitude to my family, in specific my parents, Mr. Altaf Mohiuddin Syed and Mrs. Sufiya Syeda for providing me with unfailing support and continuous encouragement throughout career. I owe my success to them.

Finally, I thank all my friends for their moral support, which helped me achieve this success

Abstract

Exploration and optimization of different designs inspired by naturally existing forms and patterns together proving those structures being structurally stable is a continuous and iterative procedure. Manual approaches to the exploration of any type of structure are time-consuming and could lead to erroneous solutions. On the other hand, the parts of the structure, for example, metal sheet panels that form the shell structure is expected to be efficiently manufactured, i.e., the cutting of panel geometry should be well planned to avoid higher material wastages.

Evolutionary solving techniques developed based on Darwin's theory of natural evolution serves as an incredible method helpful for the exploration and optimization of designs. Therefore, this research study focusses merely on two main objectives, i.e., one directed towards the design exploration of shell structure proving to be stable and the other directed towards the efficient manufacturing of metal panels that form the shell structure.

The mathematical formulations for developing a shell surface in the form of algorithm is extensively inspired from the pre-historic ideas of shell surface developments and Voronoi pattern available in the natural existing surfaces. The manufacturing techniques of metal sheet panels are also understood before applying the genetic algorithm for panel packing.

Chapter 2 of this research study explains the concepts for the generation of NURBS which are required for the generation of the free form shell surface along with the concepts on Voronoi tessellation and its relaxation. The practices in metal sheet façade manufacturing are also explained.

Chapter 3 presents the implementation of the concepts of design optimization of free form shell structure in Grasshopper using the genetic algorithm. Besides, the genetic algorithm is applied to obtain the optimized panel distribution in an assumed metal sheet area.

Chapter 4 presents the results for the implemented algorithm for both the objectives of this research study.

Chapter 5 presents the conclusions and outlook of the research study.

Table of Contents

Task Sheet.....	II
Declaration.....	III
Acknowledgement	IV
Abstract.....	V
Table of Contents	VI
List of Figures.....	VIII
List of Tables	XI
List of Abbreviations	XII
1 Introduction.....	1
1.1 Motivation.....	1
1.2 The Objective of the Study	2
1.3 Problem Statement	3
1.4 Organization of Thesis	3
2 Background and Related Work.....	4
2.1 Freeform Architecture.....	4
2.2 Shell Structures	4
2.2.1 Historical Development	4
2.2.2 Types of Shell Structures	5
2.3 Generation of NURBS	6
2.3.1 Introduction to Splines	6
2.3.2 Mathematical Form- Power Basis Form of a Curve	7
2.3.3 Non-Uniform Rational Basis Spline Surfaces [NURBS].....	8
2.4 Voronoi Diagram	11
2.4.1 Introduction.....	11
2.4.2 Concept of Voronoi Generation.....	11
2.4.3 Properties of Voronoi Diagram.....	12
2.4.4 Types of Algorithm.....	12
2.4.5 Voronoi Pattern Relaxation-Lloyd’s Algorithm	14
2.5 Practices in Metal Sheet Facade Manufacturing	15
2.6 Genetic Algorithm	17
2.6.1 Introduction.....	17
2.6.2 Concept of Genetic Algorithm.....	18

2.7	Case Studies	22
2.7.1	The BUGA Wood Pavillion	22
2.7.2	Soumaya Museum	26
3	Methodology for Optimization Process.....	30
3.1	Optimization of Shell Structure Form - Structural Stability	30
3.1.1	Creation of 3D Shell Surface with Voronoi Pattern.....	30
3.1.2	Basic Structural Analysis for Fitness Value.....	43
3.2	Optimization of Cell or Panel Packing.....	46
4	Results and Discussion.....	51
4.1	Optimization of Shell Structure Form - Structural Stability	51
4.1.1	Case 1: Form with Single Opening and Irregular Voronoi Tessellation.....	51
4.1.2	Case 2: Form with Single Opening and Relaxed Voronoi Tessellation.....	53
4.1.3	Case 3: Form with Double Openings and Relaxed Voronoi Tessellation.....	56
4.2	Optimization of Cell or Panel Packing.....	58
4.2.1	Case 1: Panel Packing for Low Level of Tuning	58
4.2.2	Case 2: Panel Packing for High Level of Tuning	60
5	Conclusions and Future Work.....	62
5.1	Conclusions.....	62
5.2	Future work.....	65
	Bibliography	66
	Appendix.....	69

List of Figures

Figure 1.1: Evolution of structural systems in time [23]	1
Figure 1.2: The BUGA Wood Pavilion [18].....	2
Figure 2.1: A Hanging model of Gaudí reconstructed by a team from Stuttgart, based on Frei Otto and Tomlow, scale. The model is now in the museum of the Sagrada Família. Photo: wiki.	5
Figure 2.2: Model of a ruled surface, also to be seen in the museum of the Sagrada Família. Photo: Silke Scheerer	5
Figure 2.3: TWA Terminal in 1962 (Example of Thin Shell Structure) [7]	6
Figure 2.4: Sydney Opera House in 1957 (Example of Thick Shell Structure) [8]	6
Figure 2.5: Spline of first degree	7
Figure 2.6: Spline of third degree	8
Figure 2.7: 3 rd Degree Bézier curve [2]	9
Figure 2.8: Circle arc, defined using weights [2].....	9
Figure 2.9: Voronoi in Nature [24] and [25].....	11
Figure 2.10: Voronoi Diagram for irregular point distribution [2]	11
Figure 2.11: Voronoi diagram for regular distribution	12
Figure 2.12: Circle passing through three sites.....	12
Figure 2.13: Fortune's Sweep Line Algorithm [2]	13
Figure 2.14: Points on Circle	13
Figure 2.15: Circumcircles drawn from different sites	13
Figure 2.16: Voronoi diagram by Delaunay triangulation	13
Figure 2.17: Iteration 1	15
Figure 2.18: Iteration 2	15
Figure 2.19: Iteration 7	15
Figure 2.20: Iteration 45(Algorithm stopped).....	15
Figure 2.21: Types of cutting practices.....	15
Figure 2.22: Types of bending practices.....	16
Figure 2.23: (i) Bottoming, (ii) Air bending, (iii) Coning	17
Figure 2.24: Springback effect.....	17
Figure 2.25: Five phases of genetic algorithm.....	18
Figure 2.26: Definition of population	18
Figure 2.27: Exchanging genes between two parents A1 and A2.....	20
Figure 2.28: New Offspring	20
Figure 2.29: Uniform Crossover	20
Figure 2.30: Mutation Before and After	20
Figure 2.31: South-View of BUGA Wood Pavilion, © ICD/ITKE University of Stuttgart [19]	22

Figure 2.32: Interior and flexible event space.....	22
Figure 2.33: Multidisciplinary process © ICD/ITKE University of Stuttgart [19].....	23
Figure 2.34: Structural study [11].....	23
Figure 2.35: Parts involved in a panel [11].....	24
Figure 2.36: Robotics involved during the fabrication process [11].....	24
Figure 2.37: Soumaya Museum, Mexico ©Adam Weisman [26].....	26
Figure 2.38: Soumaya Museum, Mexico ©Rafael Gamo [26].....	26
Figure 2.39: Layers during construction [28].....	27
Figure 2.40: Layers considered [27].....	27
Figure 2.41: Hexagons enclosed by intersecting circles [21].....	28
Figure 2.42: Hexagon diameter and gap [21].....	28
Figure 2.43: Vertical curves to stretch hexagons [21].....	28
Figure 2.44: Stages in stretching [21].....	28
Figure 2.45: Final panel families [15].....	29
Figure 2.46: Construction process [15].....	29
Figure 3.1: Optimization process for stable structure.....	30
Figure 3.2: Polygon component in Grasshopper.....	31
Figure 3.3: Reference plane and polygon.....	31
Figure 3.4: Creating an Ellipse at certain height.....	32
Figure 3.5: Visualization of Ellipse in Rhino.....	32
Figure 3.6: Process for geometry division.....	33
Figure 3.7: Output after division of geometry.....	33
Figure 3.8: Creating a list of points for NURBS curve.....	34
Figure 3.9: Rhino visualization of NURBS curve.....	35
Figure 3.10: Rhino visualization for Patch surface.....	36
Figure 3.11: Voronoi visualization in Rhino.....	37
Figure 3.12: Trimming the regions of Voronoi.....	38
Figure 3.13: Projecting Voronoi panels with reduction in curvature.....	39
Figure 3.14: Closing naked edges.....	39
Figure 3.15: Dimensions of panels on the shell structure.....	40
Figure 3.16: Setting offset of edges.....	40
Figure 3.17: Algorithm for Voronoi relaxation.....	41
Figure 3.18: Relaxed Voronoi pattern-Rhino.....	41
Figure 3.19: Flatness check.....	42
Figure 3.20: Centre of gravity of each panel and panel numbering (Top View).....	42
Figure 3.21: Line to Beam.....	43
Figure 3.22: Defining loads.....	44

Figure 3.23: Defining Joint	44
Figure 3.24: Defining material and cross-section	44
Figure 3.25: Defining supports	45
Figure 3.26: Model assembly and analysis	45
Figure 3.27: Visualization of stress distribution in the model	46
Figure 3.28: Random picking of Voronoi cells for nesting	47
Figure 3.29: Generation of random points and sheet	47
Figure 3.30: Transferring panels from 3D surface.....	48
Figure 3.31: Collision check and fitness value generation	49
Figure 3.32: Measuring dimensions of panels on 2D sheet	49
Figure 3.33: Visualization of dimensions (Not optimized).....	49
Figure 3.34: Internal angular measurement	50
Figure 3.35: Visualization of internal angles	50
Figure 4.1: Galapagos component in Grasshopper	51
Figure 4.2: Algorithm output graphs for Case 1	53
Figure 4.3: Algorithm visual output for Case 1	53
Figure 4.4: Algorithm output graphs for Case 2	55
Figure 4.5: Algorithm visual output for Case 2	55
Figure 4.6: Algorithm output graphs for Case 3	57
Figure 4.7: Algorithm visual output for Case 3	57
Figure 4.8: Final structure after visualization	58
Figure 4.9: Inputs for solver.....	58
Figure 4.10: Initial packing of panels	59
Figure 4.11: Final packing of panels for case 1	59
Figure 4.12: Inputs for solver.....	60
Figure 4.13: Final packing of panels for case 2 (not to scale)	61

List of Tables

Table 2.1: Characteristics of cutting technologies	16
Table 3.1: Inputs for polygon component.....	31
Table 3.2: Outputs from polygon component	31
Table 3.3: Inputs for Ellipse component.....	32
Table 3.4: Output from Ellipse component.....	32
Table 3.5: Input for Ellipse Segmentation	33
Table 3.6: Input for Base Geometry Segmentation.....	33
Table 3.7: Inputs for NURBS curve component.....	35
Table 3.8: Output from NURBS Component.....	35
Table 3.9: Inputs for Patch component	35
Table 3.10: Output from Patch component.....	36
Table 3.11: Inputs for Population component.....	36
Table 3.12: Outputs from Population component.....	37
Table 3.13: Inputs for Voronoi component.....	37
Table 3.14: Output from Voronoi component	37
Table 4.1: Geometrical inputs for Case 1	51
Table 4.2: Inputs for Genetic algorithm of Case 1 (Galapagos)	52
Table 4.3: Geometrical inputs for Case 2	54
Table 4.4: Inputs for Genetic algorithm of Case 2 (Galapagos)	54
Table 4.5: Geometrical inputs for Case 3	56
Table 4.6: Inputs for Genetic algorithm of Case 3 (Galapagos)	56
Table 4.7: Parameters as a gene pool for Galapagos	58
Table 4.8: Centroidal co-ordinates and rotation angles of panels for initial packing configuration	59
Table 4.9: Centroidal co-ordinates and rotation angles of panels for final packing configuration	59
Table 4.10: Parameters as a gene pool for Galapagos	60
Table 4.11: Centroidal co-ordinates and rotation angles of panels for initial packing	60
Table 4.12: Centroidal co-ordinates and rotation angles of panels for final packing	61

List of Abbreviations

CVTs	Centroidal Voronoi Tessellations
DG	Delaunay Graph
Eq.	Equation
GA	Genetic Algorithm
ICD	Institute of Computational Design and Construction
ITKE	Institute of Building Structures and Structural Design
LVL	Laminated Veneer Lumber
MDS	Master Design Surface
NURBS	Non-Uniform Rational Basis Splines Surfaces
TWA	Trans World Airlines

1 Introduction

1.1 Motivation

In the past decade, freeform architecture has enormously overtaken the construction sector all around the globe. Architects are engaging to reveal new and complex ideas of design inspired by the patterns available in nature. Meanwhile, this inspiration influenced the construction engineering division to arise with lightweight, structurally stable and economical structures. The novel thoughts of architectural and civil engineering fields were stimulated by the transformations considered concerning science, innovative new materials, digitalization and manufacturing processes[1].

Figure 1.1 explains the evolution of structural systems over the years, i.e. forms of architectural structures during the start of civilization to the current trends of digital free-form structures. It can be noticed that the weight of the structure from the beginning has tremendously changed into lightweight structures with considerable changes in structural stability (see Figure 1.2).

Besides, in the 20th century, the digital revolution radically restructured different industries in the global market. Engineers observed the benefits and explored the digital processes in manufacturing techniques for fabricators and contractors. One of the biggest advantages was to control the manufacturing information resulting in inaccurate material and cost estimates. This digital revolution was immensely beneficial over the normative practices which were erroneous and time-consuming. This revolution also helped the architects to study the different free-form structures with less manpower, material, money and time.

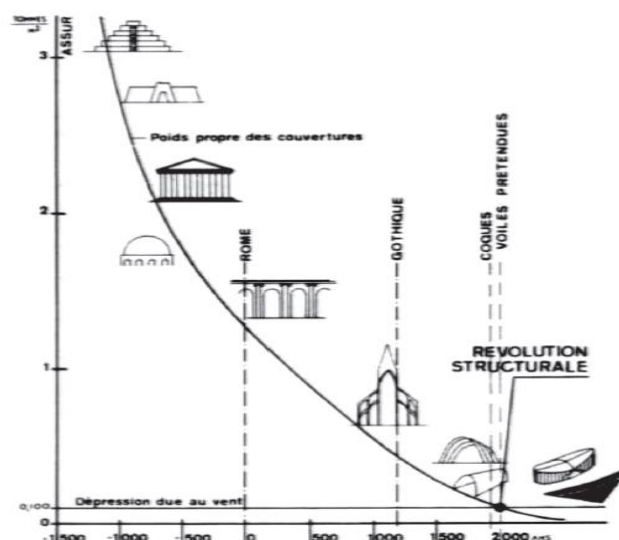


Figure 1.1: Evolution of structural systems in time [23]



Figure 1.2: The BUGA Wood Pavilion [18]

1.2 The Objective of the Study

This research study includes two main objectives and is briefly mentioned below:

1. Optimization of freeform metal sheet assembled shell structure with respect to structural stability

Although the digital approaches are considered to be the most popular ones to find the different free forms and surface patterns on the structure, the manual approaches to prove those being structurally stable is not easy and accurate. The manual approaches of structural analysis with a large number of iterations having a different combination of varying parameters and constraints is time-consuming and hence digital methods of structural analysis are important. Therefore, the optimization technique of genetic algorithm is considered to obtain the optimum structurally stable free-form shell structure with varying parameters.

2. Optimization of cell or panel distribution in full-scale sheet metal for an effective manufacturing process

The metal sheet façade manufacturing industry have enormous problems dealing with the material wastages during the manufacturing process of façade panels or grid cell panels. The problem arises due to the requirements of irregularly shaped panels by unconventional architectural designs. The placement of each irregularly shaped panels on a full-scale metal sheet at the right position to have minimum material wastage is a great challenge. Hence, the optimization technique of genetic algorithm is considered to obtain the optimized distribution of cells or panels.

1.3 Problem Statement

This research study focuses on the following questions:

- Q1. What are freeform shell structures and what are the background concepts to achieve those?
- Q2. What geometrical aspects shall be considered to obtain highly aesthetic shell structures?
- Q3. How can a structure be optimized with respect to structural stability?
- Q4. What factors govern the structural stability and how can it be achieved in Grasshopper?
- Q5. How metal sheet panel manufacturing is carried out in the construction industry, i.e., Laser cutting, bending and joining?
- Q6. Which optimization technique can be used to achieve minimum material wastages during the manufacturing process of metal sheet panels, i.e., what parameters serve to produce optimum solution for panel distribution in a full scale of the metal sheet?

1.4 Organization of Thesis

The thesis is divided into five sections. The very first section is the introduction which includes the motivation behind choosing a specific area of research. This section also includes the research questions which are explored in this case study. The second section is the conceptual background which is split into seven parts, the background on all the concepts that are utilized to prepare the algorithm of this research work and a theoretical framework for the respective case studies. The third section corresponds to the methodology for the optimization process, which includes detailed step by step explanation of two algorithms referring to structural stability and manufacturing process respectively. The Results and discussion being the fourth section comprise of detailed analysis of various cases that demonstrate the application of a genetic algorithm for both the aims of this particular research work. The last section refers to conclusions drawn from this research work and future work that can be carried out to improve the algorithm further for various other applications.

2 Background and Related Work

2.1 Freeform Architecture

The presence of different objects in nature with a variety of free forms and patterns gives greater options for the architects to duplicate these free forms into the civil engineering structures. The free forms in nature are the structural systems that conform to a large number of complex, irregular and non-uniform forces acting on it. It is stated that throughout the years of evolution it attempts to minimize material and potential energy in the system [2]. Free form buildings are defined as building shapes with double curved shapes, which do not feature repetition of elements and of which the shape is not structurally optimised[3].

The method of obtaining such natural forms is known as the form-finding process. The form-finding has classical and modern definitions. In the former case, the process of form-finding is the relationship between the form and forces which are under static equilibrium all over the structure. But, in the latter case, the form finding process involves a description of the geometry and then identifying an appropriate architectural and structural shape.

According to research on Computational form-finding methods for fabric structure [4], form-finding is the process that determines the surface configuration of a fabric structure under pre-stress. There are a variety of numerical methods to find the forms based on the different variables and the most common methods are the transient stiffness, forced density, and dynamic relaxation methods. Although these approaches have different numerical methods and tools, which involves iterative computation process to result in a shape that is in static equilibrium.

In this research study, the form-finding process is carried out by using optimization technique - genetic algorithm to obtain the desired form of a shell structure having Voronoi pattern by setting different limitations in the parameters such as the height, width, length etc.

2.2 Shell Structures

2.2.1 Historical Development

The early intuitive ideas of developing shell structures began at the end of 17th and at the beginning of 18th centuries, where the form-finding of the structure were carried out by many processes to obtain the efficient structures.

Antoni Gaudi emerged with an idea that when a flexible rope held at two extreme ends is allowed to suspend along its self-weight [5], i.e., the catenary shape of the rope due to self-weight suspension represents the state of equilibrium in the rope which has tensile forces. Catenary represents the state of the minimal possible potential energy of the rope. The catenary can be described mathematically by a hyperbolic cosine function [6]. It holds a parabolic shape

when it adjusts itself throughout the chain due to a constant uniform load. Therefore, Antoni Gaudi made this catenary rigid and inverted about its supports to form an arch or a thrust line, only normal compressive forces occur within the cross-section. The thrust line corresponding to an applied uniform load is a quadratic parabola, it is approximately also that of a dead load of an arc with a constant cross-section. Antoni Gaudi used this concept in structural design for the crypt of the Church of Colonia Guell, Santa Coloma de Cervello near Barcelona.



Figure 2.1: A Hanging model of Gaudí reconstructed by a team from Stuttgart, based on Frei Otto and Tomlow, scale. The model is now in the museum of the Sagrada Família. Photo: wiki.

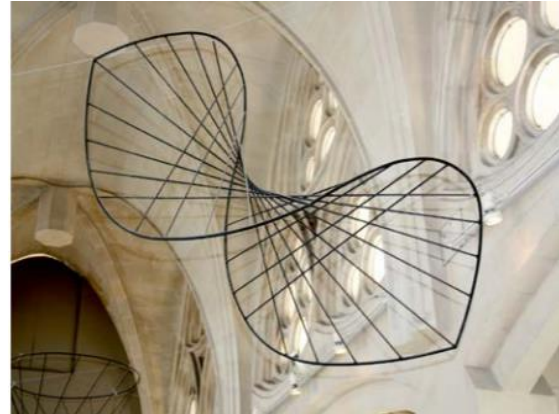


Figure 2.2: Model of a ruled surface, also to be seen in the museum of the Sagrada Família. Photo: Silke Scheerer

For the Sagrada Família, Gaudí created a hanging model consisting of wire chains and weights. They represent the main supporting links. Concerning Gaudí's view of nature, the filigree branches of the column heads, which merge into parabolic arches, in combination with the special lighting concept lend the building a unique luminosity and aesthetics. It is also interesting to note that Gaudí mainly used ruled surfaces. These double-curved surfaces have the advantage that they can be created by straight lines. Construction began in 1882 and continues to this day.

Later in the year 1950, Swiss engineer Heinz Isler utilized physical models to create a three-dimensional surface with the method of hanging models. The form the structure assumed was an incredible achievement by Isler. These models when inverted or flipped along the supports led to a freeform shell structure involving compressive forces.

2.2.2 *Types of Shell Structures*

When designing a civil engineering structure, it is foremost important to understand the flow of forces and choose appropriate materials for load-bearing actions. The definition of shell structure represents that it is a type of building construction which has thin, curved plate structures shaped to transmit forces by compressive, tensile and shear stresses that act in the

plane of the surface. The thickness of the shell is very small in comparison with the other dimensions.

There are different types of shell structures as mentioned below;

- Shell Barrel Vaults
- Multi-Bay Barrel Vaults
- Corrugated Barrel Vaults
- Saddle shell
- Hyperboloids of Revolution
- Thin Shell Structures
- Thick Shell Structures
- Shell Dome
- Gird Shell



Figure 2.3: TWA Terminal in 1962 (Example of Thin Shell Structure) [7]



Figure 2.4: Sydney Opera House in 1957 (Example of Thick Shell Structure) [8]

Based on the engineering concepts developed for the shell structures, this research work is directed towards applying these developed concepts into modern methods of the optimization process to achieve an appreciably aesthetic structure with proof of being structurally stable. Therefore, modern optimization method of evolutionary algorithm known to be a Genetic algorithm is used and is as explained further.

2.3 Generation of NURBS

The term NURBS (Non-Uniform Rational Basis Splines Surfaces) was derived by the principle developed by Pierre Bézier, and Paul de Casteljaou for the polynomial representation of curves. To understand the mathematical formulations for the generation of NURBS, it is necessary to go through a few basic ideas about the splines and its forms.

2.3.1 Introduction to Splines

Splines are piecewise polynomial curves, which are easy to construct, accurate to evaluate and can approximate the complex shapes through curve fitting, i.e., a spline function consists of

polynomial pieces on subintervals joined together with certain continuity conditions. The points where the segments connect are called as the knots of the spline.

2.3.2 Mathematical Form- Power Basis Form of a Curve

Considering available points as $x_0, x_1, x_2, x_3, \dots, x_n$ holds a condition $x_0 < x_1 < \dots < x_n$. In addition, considering an integer value $k \geq 0$. Then, the spline function of degree p having knots $x_0, x_1, x_2, x_3, \dots, x_n$ is a function S such that[9]:

- (1) on each interval $[x_{i-1}, x_i]$, S is a polynomial of degree $\leq k$;
- (2) S has a continuous $(k-1)^{\text{st}}$ derivative on $[x_0, x_n]$.

Here, S is a piecewise polynomial of degree p having continuous derivative of all orders up to $(k-1)$.

- A spline of degree 1 or linear spline is represented as follows;

$$S(x) = \begin{cases} p_1(x) = a_1 + b_1x, & x \in [x_0, x_1], \\ p_2(x) = a_2 + b_2x, & x \in [x_1, x_2], \\ \vdots & \vdots \\ p_n(x) = a_n + b_nx, & x \in [x_{n-1}, x_n] \end{cases} \quad (\text{Eq. 1})$$

where, $a = x_0 < x_1 < \dots < x_n = b$, the linear spline $S(x)$ is a continuous function that interpolates the data and is constructed from linear functions that are two-point interpolating polynomials.

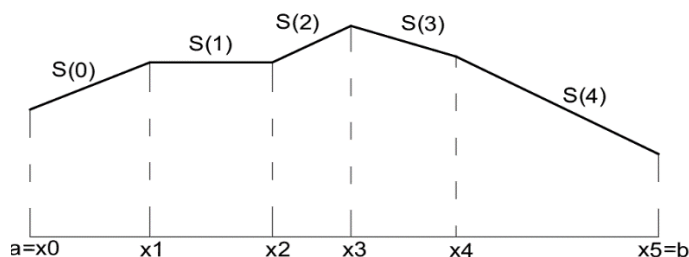


Figure 2.5: Spline of first degree

- A spline of degree 2 or a quadratic spline is represented as follows;

$$S(x) = \begin{cases} p_1(x) = a_1 + b_1x + c_1x^2, & x \in [x_0, x_1], \\ p_2(x) = a_2 + b_2x + c_2x^2, & x \in [x_1, x_2], \\ \vdots & \vdots \\ p_n(x) = a_n + b_nx + c_nx^2, & x \in [x_{n-1}, x_n] \end{cases} \quad (\text{Eq. 2})$$

where, $a = x_0 < x_1 < \dots < x_n = b$, the spline $S(x)$ is a continuous function that interpolates the data and is constructed from piecewise quadratic polynomial functions.

- A spline of degree 3 or a cubic spline is represented as follows;

$$S(x) = \begin{cases} p_1(x) = a_1 + b_1x + c_1x^2 + d_1x^3, & x \in [x_0, x_1], \\ p_2(x) = a_2 + b_2x + c_2x^2 + d_2x^3, & x \in [x_1, x_2], \\ \vdots & \vdots \\ p_n(x) = a_n + b_nx + c_nx^2 + d_nx^3, & x \in [x_{n-1}, x_n] \end{cases} \quad (\text{Eq. 3})$$

where, $a = x_0 < x_1 < \dots < x_n = b$, the spline $S(x)$ is a continuous function that interpolates the data and is constructed from piecewise cubic polynomial functions. In Figure 2.6, the black points with straight lines represent the control points with which the curvature of the spline can be controlled.

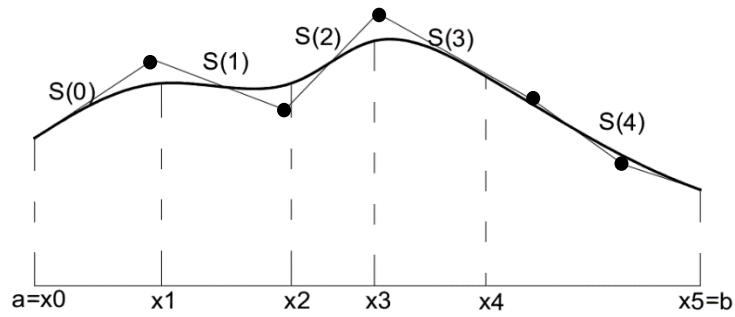


Figure 2.6: Spline of third degree

2.3.3 Non-Uniform Rational Basis Spline Surfaces [NURBS]

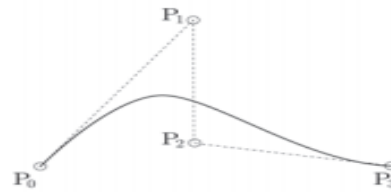
As the Power basis curves are unnatural for interactive shape design. Bézier curves were developed as a mathematically equivalent form, yet more suitable for geometric modelling, i.e., manipulation of the shape with the use of a computer. As per [2], the problem of generalization of Bézier splines to create non-uniform, rational B-Splines helped into the generation of Non-Uniform Rational Basis Spline surfaces, or NURBS surfaces. The generation of NURBS was carried out as mentioned below [9]:

The general form of an n^{th} degree Bézier curve is:

$$S(x) = \sum_{i=0}^n B_{i,n}(x) P_i, \quad 0 \leq x \leq 1 \quad (\text{Eq. 4})$$

Bézier introduced two important ingredients such as P_i (vector of control points) and a basic function $B_{i,n}(x)$. The P_i is represented over coordinates in space $P_i = (x_i, y_i, z_i)$ and basis functions are known as Bernstein polynomials of degree n :

$$B_{i,n}(x) = \frac{n!}{i!(n-i)!} x^i (1-x)^{n-i}, \quad 0 \leq x \leq 1 \quad (\text{Eq. 5})$$

Figure 2.7: 3rd Degree Bézier curve [2]

As seen in the figure, the 3rd-degree Bézier curve includes P_0 , P_1 , P_2 and P_3 represent control points, and the polygon between them represents the approximated shape of the curve and is represented by;

$$S(x) = (1 - x)^3 P_0 + 3x(1 - x)^2 P_1 + 3x^2 (1 - x) P_2 + x^3 P_3 \quad (\text{Eq. 6})$$

Rational Bézier Curves: The concept of weights was introduced, as the Bézier Curves cannot be used to precisely represent conic sections (like circles, ellipses, hyperbolas, spheres, etc.) using polynomials[2]. If there is a weight vector $\{w_i\}$, the n^{th} degree rational Bézier curve can be expressed as:

$$S(x) = \frac{\sum_{i=0}^n B_{i,n}(x) P_i w_i}{\sum_{i=0}^n B_{i,n}(x) w_i}, \quad 0 \leq x \leq 1 \quad (\text{Eq. 7})$$

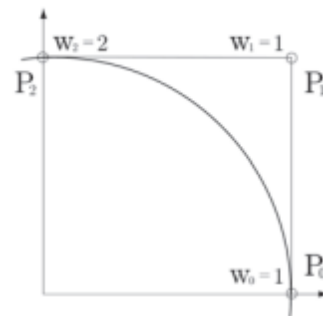


Figure 2.8: Circle arc, defined using weights [2]

A simple quarter of a circle (see Figure 2.8) is represented by a factor (a number) that will pull the curve toward the control point (hence named as weight), thus these weights help in additional control for correcting the curves.

B-Spline Curves: To generate the B-spline curves, there is a need for combining B-spline Basis function with n Bézier curves into one expression

$$S(x) = \sum_{i=0}^n N_{i,p}(x) P_i, \quad a \leq x \leq b \quad (\text{Eq. 8})$$

where, P_i is a control point vector and $N_{i,p}(x)$ represents p^{th} degree B-Spline basis functions, defined over a specific nonperiodic (and non-uniform) knot vector X :

$$X = \{a, \dots, a, x_{p+1}, \dots, x_{m-p-1}, b, \dots, b\} \quad (\text{Eq. 9})$$

The definition of i^{th} B-Spline basis function of p -degree (order $p + 1$) over a knot vector $X = \{x_1, \dots, x_n\}$ is expressed as [9]:

$$N_{i,0}(x) \begin{cases} 1 & \text{if } x_i \leq x \leq x_{i+1} \\ 0 & \text{otherwise} \end{cases} \quad (\text{Eq. 10})$$

$$N_{i,p}(x) = \frac{x - x_i}{x_{i+p} - x_i} N_{i,p-1}(x) + \frac{x_{i+p+1} - x}{x_{i+p+1} - x_{i+1}} N_{i+1,p-1}(x) \quad (\text{Eq. 11})$$

Rational B-Spline Curves and Surfaces: NURBS curve of p^{th} degree is obtained by introducing rational functions and weight into B-Splines as introduced previously in rational Bézier curves is as mentioned below [9];

$$S(x) = \frac{\sum_{i=0}^n N_{i,p}(x) P_i w_i}{\sum_{i=0}^n N_{i,p}(x) w_i}, \quad a \leq x \leq b \quad (\text{Eq. 12})$$

where, P_i , w_i and $N_{i,p}(x)$ represents control points, weights and a p^{th} degree B-Spline basis function respectively over a specific non-periodic and non-uniform knot vector X .

Generating a NURBS surface is carried out by including another parameter v for the second direction, together with its B-Spline basis function and its knot vector. A NURBS surface of degree p in u direction and degree q in the v direction as a piecewise rational polynomial function is represented by the following equation [9];

$$S(u, v) = \frac{\sum_{i=0}^n \sum_{j=0}^m N_{i,p}(u) N_{j,q}(v) P_{i,j} w_{i,j}}{\sum_{i=0}^n \sum_{j=0}^m N_{i,p}(u) N_{j,q}(v) w_{i,j}}, \quad 0 \leq u, v \leq 1 \quad (\text{Eq. 13})$$

where, $P_{i,j}$ represents a network of control points in two directions (i, j), $w_{i,j}$ represents their weights and their respective non-rational B-Spline basis functions in two directions are $N_{i,p}(u)$ and $N_{j,q}(v)$ defined over two knot vectors U and V .

2.4 Voronoi Diagram

2.4.1 Introduction

This is a unique method of space decomposition, which was invented over 100 years ago by a professor at the University of Warsaw known as Georgy Voronoi [2]. It is also known as Voronoi decomposition or Voronoi tessellation. As per [10], Voronoi diagrams are a method of spatial data interpolation into polygons around each point in such a way, that each location from the area surrounding a given point is closer to it than to any other point. The Voronoi pattern is available in several objects in nature. Figure 2.9 shows the availability of Voronoi pattern in a leaf and wing of Dragonfly.

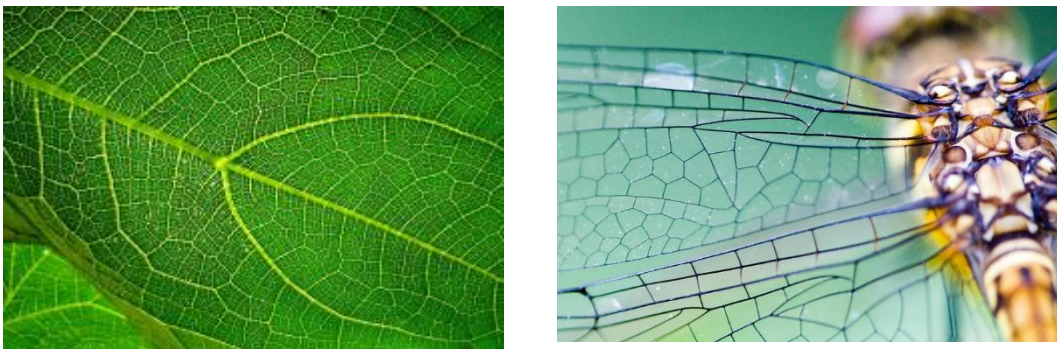


Figure 2.9: Voronoi in Nature [24] and [25]

2.4.2 Concept of Voronoi Generation

A typical Voronoi tessellation created on a 2D surface with a set of points distributed randomly (Voronoi seeds) is as shown in Figure 2.10. There is a set of points $P = \{p_1, p_2, \dots, p_n\}$ in a plane. With the help of Euclidean distance measurement, the distance between the two points is measured, i.e., the distance of each point from other points is measured and the points closest to a particular point belongs to that specific point/site. The bisector line is drawn at the centre position of the distance measured between the points. Thus, these bisector lines form borderlines between the cells forming a Voronoi diagram. It can be noticed that the average number of edges of a Voronoi cell is less than six.

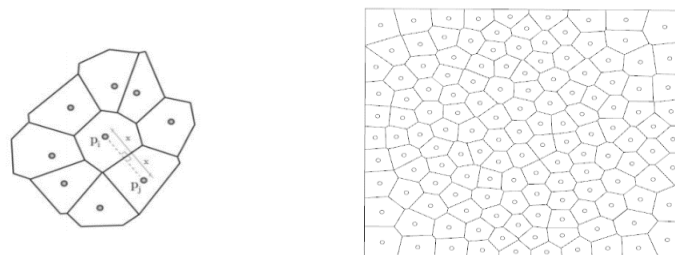


Figure 2.10: Voronoi Diagram for irregular point distribution [2]

Also, the Voronoi pattern can be generated in different forms, i.e., it is possible to be generated as a grid shell by placing the initial seeds at required distances. Some of the possible Voronoi patterns that can be generated are the triangular, quadrangular, hexagonal (see Figure 2.11) and the combinations.

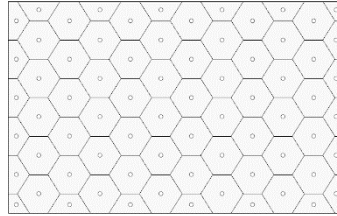


Figure 2.11: Voronoi diagram for regular distribution

2.4.3 Properties of Voronoi Diagram

1. Each point on an edge of the Voronoi diagram is equidistant from its two nearest neighbours. A circle can be drawn at the point (being the centre of the circle), where the three Voronoi cells intersect (Voronoi vertex) and this circle passes through the three points or sites. Also, this circle do not contain any other sites in its interior.

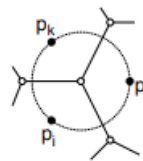


Figure 2.12: Circle passing through three sites

2. If there are 'n' number of sites, then the Voronoi diagram in a planar region has exactly n faces. Therefore, the number of Voronoi vertices is at most $2n - 5$ and the number of edges is at most $3n - 6$.

2.4.4 Types of Algorithm

There are many ways to generate the Voronoi pattern such as the Naïve $O(n^2 \log n)$ time algorithm, which works on the principles of bisector halfplanes. However, there are much more efficient ways, which run in $O(n \log n)$ time. The convex hull can be extracted from the Voronoi diagram in $O(n)$ time, it follows that this is asymptotically optimal in the worst-case [2].

- I. *Fortune's Sweep Line Algorithm*: Steven Fortune developed an algorithm that creates a Voronoi pattern $O(n \log n)$ time using a sweep line method rather than considering distances between the various sites. It is a method of developing a Voronoi pattern by sweeping a horizontal line on the plane consisting of some random points.

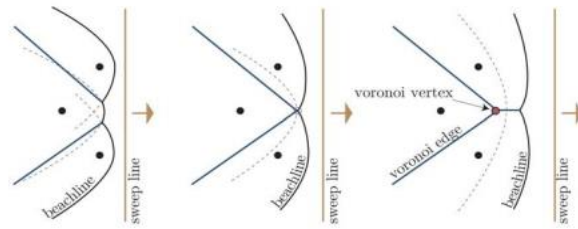


Figure 2.13: Fortune's Sweep Line Algorithm [2]

The method includes a straight line which is known as the sweep line that moves forward from left to right in the above case as shown in Figure 2.13. Considering a very simple example of having three sites. The parabolas are generated which defines the curves formed by the points that are at equal distance from the sweep line and site. A curve is formed by erasing the curves beyond the points of intersection of parabolas (See beachline). The blue line represents the emerging Voronoi diagram and the red point represent the Voronoi vertex created due to the three sites. The process is continued until all the sites are swept.

- II. *Delaunay triangulation*: It is defined by the terms of an empty circumcircle property for triangle[11]. It is a unique circumcircle which passes through the three points or vertices of a triangle, .i.e. the points of the triangle lie on the circumference of the circle as shown in Figure 2.14.



Figure 2.14: Points on Circle

Considering a finite set of points in P and if the circumcircle of every triangle is empty, .i.e., when there is no point of set $P = \{x_1, x_2, x_3, x_4, x_5, x_6, x_7\}$ in the interior of the circumcircle then, it is known as Delaunay triangulation. In the below example it can be seen that circumcircles of all the 7 triangles are empty.

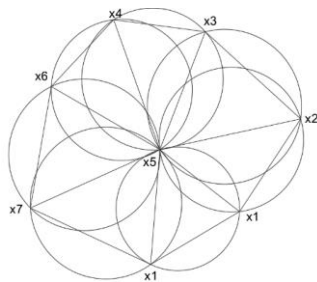


Figure 2.15: Circumcircles drawn from different sites

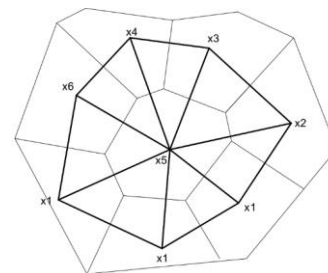


Figure 2.16: Voronoi diagram by Delaunay triangulation

There is a one-to-one correspondence between the bounded cells and the vertices of V or (P) that makes its dual graph – Delaunay graph $DG(P)$. Nodes of this graph serve as sites for the Voronoi diagram and it has an edge between two sites which is common to both the sites (See Figure 2.16). Following the simple example of a set of eight points P , where the points represent sites, dull lines representing the Voronoi diagram and bold lines its dual graph, the Delaunay triangulation. This method of creating triangulation was invented by, and named after a Russian mathematician Boris Delaunay[2].

Some of the characteristics of 2D planar division are as follows,

- No two edges ever cross each other - it is a plane graph.
- The circumcircle of any triangle in a Delaunay triangulation contains no point of P in its interior.
- Every Delaunay triangulation of P maximizes the smallest angle overall triangulation of P .
- Each vertex has on average six surrounding triangles

The method with which the Grasshopper component creates the Voronoi tessellation is based on Delaunay triangulation and it is therefore used in the research work.

2.4.5 Voronoi Pattern Relaxation-Lloyd's Algorithm

Lloyd's algorithm is one of the most popular iterative schemes for computing the centroidal Voronoi tessellations. As per research on Lloyd's algorithm [12], Centroidal Voronoi tessellations (CVTs) are Voronoi tessellations of a bounded geometric domain such that the generating points of the tessellations are also the centroids (mass centres) of the corresponding Voronoi regions with respect to a given density function. It is stated that every time a relaxation step is performed, the points are left in a slightly more even distribution, i.e., closely spaced points move farther apart, and broadly spaced points move closer together[13].

The algorithm aims to bring the centroids of the Voronoi cells and points of the k sites position close to each other by the repetitive procedure. It starts by considering several k points or sites as mentioned in the above section 2.4.2 to create Voronoi pattern, i.e., randomly distributed points that are used to populate the surface.

1. Once the centroids of the created Voronoi cells are calculated, these centroids act as new sites for the cells and hence new Voronoi cells are created.
2. The above step is repeated until the centroid remains in the same position or there is no considerable change in the shape of the Voronoi cells.

A test example below shows relaxed Voronoi pattern created with 20 sites. Where red cross represents the original sites given to create Voronoi pattern for that particular iteration. Green cross represents the calculated centroids of cells in each iteration.

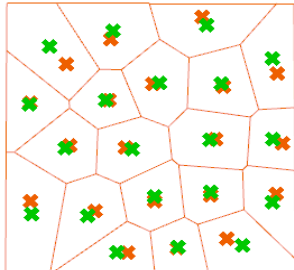


Figure 2.17: Iteration 1

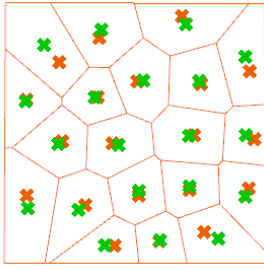


Figure 2.18: Iteration 2

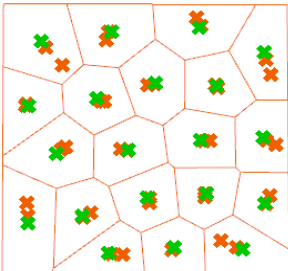


Figure 2.19: Iteration 7

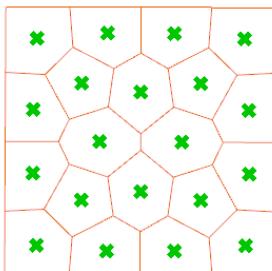


Figure 2.20: Iteration 45 (Algorithm stopped)

It can be noticed in Figure 2.20, the Voronoi tessellation is relaxed with subsequent proportional cells in comparison with the cells in other iterations (see Figure 2.17, Figure 2.18, and Figure 2.19). Thus, repositioning the centroids based on the Voronoi cells helps in generating a better pattern that can be utilized for further applications.

2.5 Practices in Metal Sheet Facade Manufacturing

According to the Fractory [14], the following mentioned or near to similar practices are carried out in the market to produce regular metal façade panels based on the raw data given. One of the main aims of this research work is the optimized cutting pattern for metal sheet manufacturing and hence it is necessary to understand the current practices of cutting in the manufacturing industry. As per technical details, there are five main methods of the metal sheet cutting and are as mentioned below;

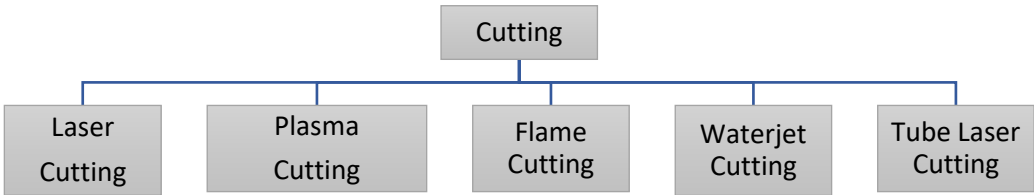


Figure 2.21: Types of cutting practices

It is stated that these cutting technologies allow greater flexibility, accuracy and top-quality cuts for both simple and complex shapes. The materials that can be cut using these techniques are carbon steel,

stainless steel, aluminium, brass, copper and titanium. The limitation of using a specific cutting technology depends on the thickness of the material considered in the project (see Table 2.1).

Table 2.1: Characteristics of cutting technologies

Technique	Material	Limits
Laser cutting	Carbon Steel	< 25 mm
	Stainless Steel	< 30 mm
	Aluminium	< 30 mm
	Copper Alloys	< 12 mm
Plasma Cutting	Carbon Steel	50 mm
	Stainless Steel	50 mm
	Aluminium	40 mm
Flame Cutting	Carbon Steel	150 mm
Waterjet Cutting	Carbon Steel	Up to 300 mm
	Stainless Steel	Up to 300 mm
	Aluminium	Up to 300 mm
Tube Laser Cutting	Carbon Steel	12 mm
	Stainless Steel	8 mm
	Aluminium	1 mm

When working with a higher level of details, it is necessary to detail the joints of the metal sheets, bending angles etc. hence, to obtain the correct angles of bend in the metal sheet assembly, there should be a proper match between the data obtained from the 3D drawing and the panels cut on the metal sheet, i.e., there should be a data signifying sufficient offsets and complete bending lines corresponding to the position of the sheet in the structure. Therefore, understanding the type of bending techniques is necessary and hence a brief explanation is mentioned below;

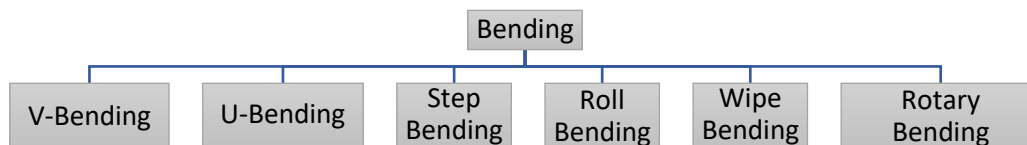


Figure 2.22: Types of bending practices

The most common type of bending technique is the V-bending, which has three sub-groups (i) bottoming, (ii) air bending, and (iii) coning. It is stated that 90 percent of the bending task is carried out using air bending and bottoming. The amount of force or tonnage required depends on the thickness of the material used and the inner radii.

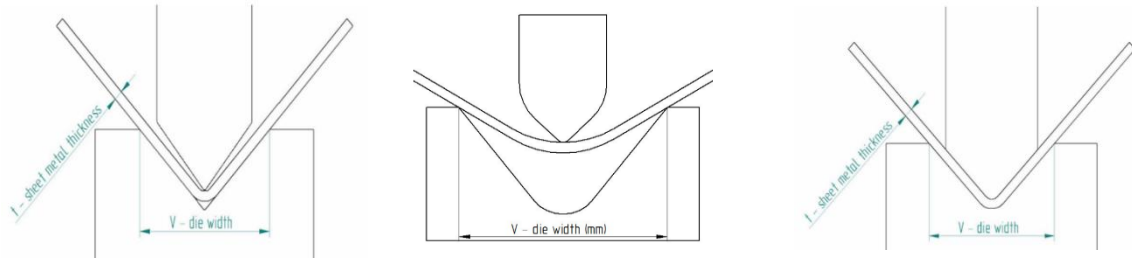


Figure 2.23: (i) Bottoming, (ii) Air bending, (iii) Coning

It is stated that carrying out bending with the above-mentioned techniques need to be accounted for bending spring back. It is nothing but natural spring back by a certain angle when the material that is being bent is withdrawn from the load. Hence, to overcome the error due to spring back, the angle of bent is added with the spring back angle to achieve the desired angle (see Figure 2.24). The bending radius also has considerable impact on the spring-back effect and it is therefore mentioned that larger the bending radius greater the spring back effect and vice versa.

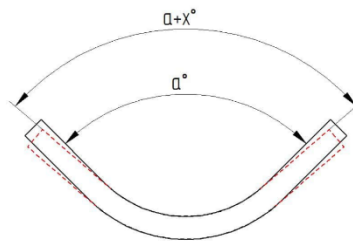


Figure 2.24: Springback effect

Based on all the above mentioned basic ideas about bending and cutting, this research work is being carried for metal panel distribution for a low level of detail representing only cutting geometry and no assembly and bending techniques are taken into consideration due to the limited scope of work in this area.

2.6 Genetic Algorithm

2.6.1 Introduction

A genetic algorithm is a search heuristic technique that comes under probabilistic methods of optimization that rely on random selection factors and probabilistic decision. It is a method that is developed based on the naturally observed phenomena. It works on the basic principle originated from Nature and its selection method influenced by Charles Darwin's theory of natural evolution.

According to [15], life was sustained through the reproduction of the first amoebas. It means the reproduction process is nothing but the multiplication process. Small random mutations started resulted in combination with the environment and were responsible for the creation of unique individuals. Some individuals survive for a longer time and some for the shorter time and this is based on how fit a particular individual is. This process is being carried out in nature to date.

2.6.2 Concept of Genetic Algorithm

Genetic algorithm is a random-based classical “Evolutionary algorithm” The basic working principle of Genetic Algorithms has one to one correspondence in the form of Generation, Selection, Mutation and Crossover. The process of natural selection starts with the selection of fittest individuals from a population. The offspring are produced which inherit the characteristics of the parents and will be added to the next generation. If in case, the parents have better fitness, their offspring will be better than parents and have a better chance of surviving. This process continues until a generation with the fittest individuals will be found.

There are five phases in the genetic algorithm and are as mentioned below [16];

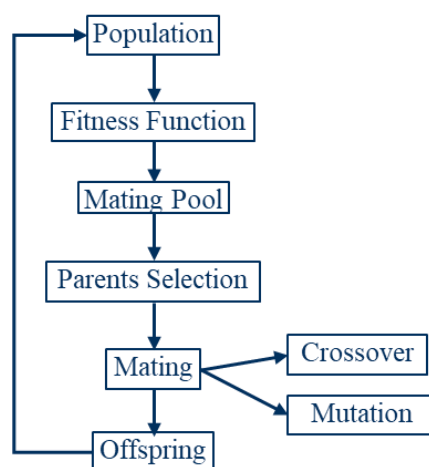


Figure 2.25: Five phases of genetic algorithm

1. *Population*: The set of individuals considered, which represents a possible solution for a problem that needs to be solved. In other words, the Genetic Algorithm works on a population consisting of some solutions where the population size is the number of solutions. Each solution is called individual and every individual is characterized by a set of parameters or variables known as Genes. Genes are joined into a string to form a Chromosome (solution). Binary values are used (a string of 1s and 0s) for encoding the genes in the chromosome. Each gene has two properties: (i) represents its value (allele) and (ii) representing the location (locus) within the chromosome which is the number above its value.

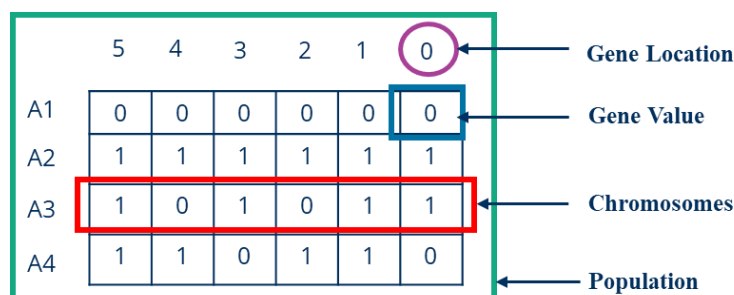


Figure 2.26: Definition of population

Each chromosome has two representations;

- (i) Genotype: The set of genes representing the chromosome.
 - (ii) Phenotype: The actual physical representation of the chromosome
2. *Fitness function*: The fitness function determines how fit an individual is in comparison with the other individuals. The result of the fitness function signifies the fitness value, which in turn represents the quality of the solution. The higher the fitness value the higher the quality of the solution. There are various kinds of fitness functions based on the objectives:
- a. Single objective fitness function
 - b. Multiple objective fitness function
3. *Selection*: In this step, the selection of two individuals is carried out based on their fitness score or quality of the solution. It is stated that selection of the best individuals based on their quality is applied to generate known as a mating pool, where the higher quality individual has a higher probability of being selected in the mating pool [17]. The selected individuals in the mating pool are the parents and the generation of two offspring are the children. The mating of high-quality individuals produces or generates increasingly higher quality individuals than their parents. Thus, eliminating lower quality individuals from generating lower quality individuals than the parents.
- Because the offspring generated using the selected parents have the same characteristics of its parents. Thus, they may include the same drawbacks as in the parents. Therefore, it shall be noted that the offspring generated with higher quality as mentioned above is possible when some changes are applied to each offspring to create new individuals. The set of all newly generated individuals will be the new population and this will replace the previously used old population. Every population created is called a generation and the process of replacing the old population by the new one is called replacement.
4. *Crossover*: It is considered to be the most significant phase in Genetic algorithm. Crossover correspondingly generates new generation as that of natural mutation. As mentioned earlier, by mutating the old generation parents, the new generation offspring arrives with genes from both the parents and the number of genes carried is random. It is essential to know that sometimes the offspring carries half of its genes from one parent and a half from the other parent. Also, the percentage of genes coming from each parent vary and it is completely random.
- a. Single point crossover: In this case, a single crossover point is chosen randomly in the chromosomes of selected two parents and genes are exchanged before and after such point from its parents. The resulting chromosomes are offspring. Thus operator is called single-point crossover (See Figure 2.27 and Figure 2.28).

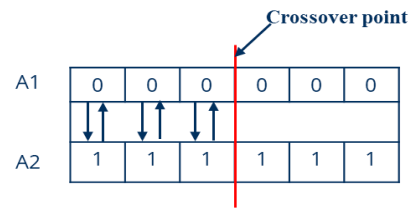


Figure 2.27: Exchanging genes between two parents A1 and A2

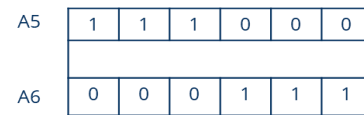


Figure 2.28: New Offspring

- b. **Two and more point's crossover:** it certainly means that the chromosomes of parents have been randomly divided into two or more parts. Thus, having two or more crossover points (See Figure 2.29). A probability factor is introduced to control the swapping of genes and to avoid the generation of the same parents again. This introduction of the probability factor is called uniform crossover [2].

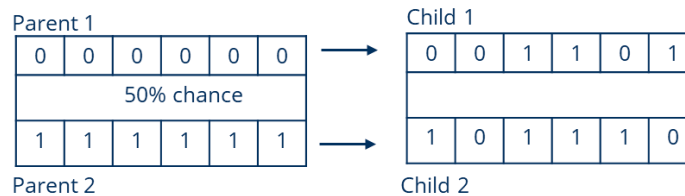


Figure 2.29: Uniform Crossover

5. **Mutation:** Swapping genes of two parents is sometimes not enough to explore the whole search space, which results in a variety of unexplored possible solutions and optimization process is in danger of easily converging to some local minimum or maximum. Therefore, to strengthen the diversity of the population, an additional factor is introduced, known as mutation. The mutation is a change, or an error in a genome, plays a secondary role, and it represents a random alteration of the single chromosome alleles. It shall be noted that without a mutation, the offspring carries all the properties of its parents. But, if there is a need to add new features to such offspring, the mutation is necessary. The mutation occurs randomly and it is therefore not recommended to increase the number of genes to be applied to mutation. The individual after mutation is called a mutant (See Figure 2.30).

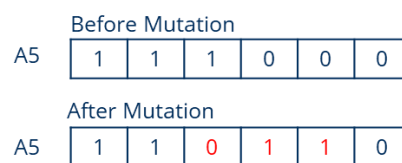


Figure 2.30: Mutation Before and After

6. **Termination:** The genetic algorithm terminates when the population has converged and does not produce offspring which are different from the previous generation. Thus, it signifies that the solution for a problem is achieved.

The optimization with the help of genetic algorithm is used in this research work to arise with the stable structure having Voronoi tessellation and is as explained in section 3.1.1 and 3.1.2. In addition, the genetic algorithm is also used for distributing and closely packing the irregular panels in the metal sheet and it is explained in section 3.2.

It is also necessary to understand the current developments taking place in the research, design and construction sectors related to this research work. Therefore, the following two cases study helps in understanding the procedures followed in each field before heading onto the preparation of optimization algorithm in grasshopper.

2.7 Case Studies

2.7.1 *The BUGA Wood Pavillion*

Reference Reason: Integrative Interdisciplinary Process in a Project

Project Name: The BUGA Wood Pavillion

Location: Central summer island of the Bundesgartenschau 2019 in Heilbronn, Germany

Contributors: The Institute of Computational design and Construction (ICD) and Institute of Building Structures and Structural Design (ITKE), University of Stuttgart, Germany

Dimensions: It spans 30 meters and covers an area of 500 m².



Figure 2.31: South-View of BUGA Wood Pavillion, © ICD/ITKE University of Stuttgart [19]



Figure 2.32: Interior and flexible event space © ICD/ITKE University of Stuttgart [19]

Inspiration: As per [18], the BUGA Wood pavilion is a segmented wood shell structure inspired by the biological principles found in the plate skeleton of the sand dollars, scientifically classified as echinoids. It is stated that the echinoid's segmented shells are an example of nature's highly efficient structures, exploiting the variation of their geometry and shapes. Thus, optimizing material and energy use. In addition, the sand dollars employ plate structures with interlocking connections between the shell's plates.

Approach: The study was conducted by the different disciplines at different phases to produce such a marvellous structure presented in the Figure 2.31 and Figure 2.32. The aim was to enable the synergistic relationships between the different disciplines i.e., the developing methods for managing the coordination across architectural design, engineering, fabrication, and assembly.

It is stated that the process was carried out by developing a computational tool based in Rhino's Grasshopper plug-in. It is stated that the main goal was to expand the scope of digital models to fabrication and construction, enabling all disciplines the possibility of checking architectural definitions against the final production geometry and construction logistics at during the process.

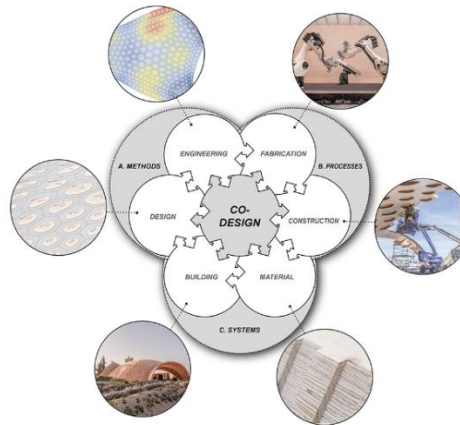


Figure 2.33: Multidisciplinary process © ICD/ITKE University of Stuttgart [19]

1. Modelling technique: Agent-based modelling was used to create the planar segmentation of the shell structure. The segments at the fold lines of the arches are stated to be following more constrained, regular arrangement and their positions were manually controlled. However, the segments of the shell's apex are said to be organised with more freedom due to actively interacting agents creating a smooth transition from a rigid grid to a less constrained segment distribution.

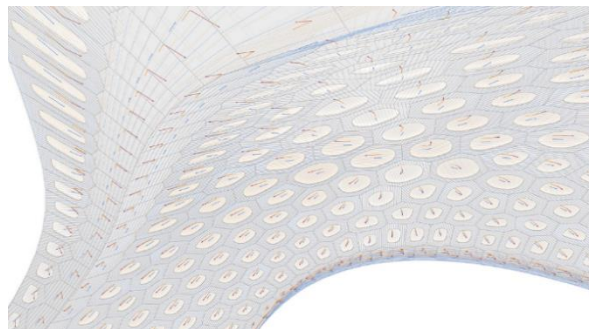


Figure 2.34: Structural study [11]

2. Materials: Wood and the plates and the beams were made of laminated veneer lumber (LVL). It uses 45 m³ of wood and the structural wooden elements weigh 36.02 kg/m².
3. Benefits of using hollow cassettes or panels: The process involved transforming the cassettes from solid plates to hollow, slicing each plate in half and embedding a ring of edge beams. Thus, improving the structural stability and it is also mentioned that it can reach a structural height of 160 mm with the same amount of material per square meter of shell surface, reaching triple the span of a shell structure with solid segments. In addition, the cavities of the shell's segments are claimed to provide very good acoustics, minimize material consumption and weight, reduce weight, and grant access inside the modules for straight forward on-site assembly.

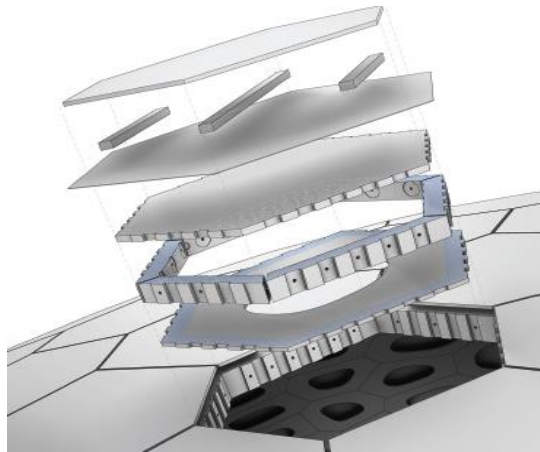


Figure 2.35: Parts involved in a panel [11]

4. The number of cassettes: Three hundred and seventy-six cassettes numbered with unique IDs.
5. Structural optimization: Information extracted for the structural design [20] from digital fabrication model includes geometry, material thicknesses of plates and beams, fibre orientation of the wood, arrangement of connection elements, and supports. Aspects studied during this step are as follows,
 - a. Influence of joint stiffness
 - b. Influence of joint tolerances
 - c. Comparison of construction systems: weight and construction height case study
 - d. Comparison of construction systems: maximum span
6. Fabrication process: Robotic fabrication process involved the following steps as mentioned in the Figure 2.36;

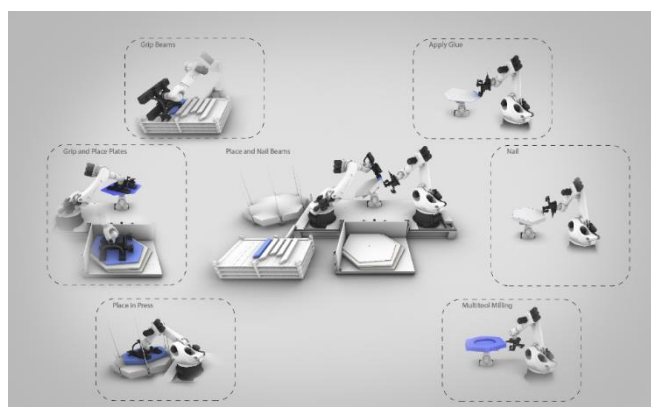


Figure 2.36: Robotics involved during the fabrication process [11]

7. On-site assembly: It is stated that the erection process was carried out in the following three stages
 - a. Spine cassettes were assembled into six assemblies of half arches and joined to three full arches with a connecting 'keystone,'

- b. The cantilever method of assembly was used for the inner shell
- c. Finally, the cassettes of the outer curves were connected to the open edges of the pavilion

The study [18] states that during the whole process there was a large amount of information related to different categories such as geometric parameters, the topological relationship with its neighbours, the final shape of its elements used for machining, the shape of its elements, different production phases, static properties, material properties, environmental and life-cycle data, connection hardware and installation constraints, fabrication data related to the robotic fabrication of the components, and information about the logistics that has been exchanged between different disciplines for successful completion of the project starting from the design phase to construction phase.

2.7.2 *Soumaya Museum*

Reference Reason: Rationalisation of freeform facades

Project Name: Soumaya Museum

Location: Mexico City, Mexico

Contributors: Fernando Romero LAR and Gehry Technologies

Dimensions: It covers an area of 17000 m².



Figure 2.37: Soumaya Museum, Mexico
©Adam Weisman [26]



Figure 2.38: Soumaya Museum, Mexico ©Rafael
Gamo [26]

This marvellous project involves façade rationalisation strategy developed by Gehry Technologies. According to a research paper [21], the strategy was carried out to mitigate the trade-offs between the project constructability i.e. having a low number of unique building components and the placement of flat hexagonal panels with perceivable irregularities of the panel-to-panel gaps on the complex surface of the structure without compromising the aesthetics of the structure. The complexity of designing, analysing and constructability of flat panels on a surface with irregular curvature is stated to be a major challenge and the different process carried out during the design and construction stages are briefly explained as the following,

It is reported that Fischer, Thomas suggested different rationalization strategies to overcome the high risk of panel fabrication economies during mass production. The three strategies considered are as follows,

- a. Pre-rationalization: Opportunities in decision making
- b. Post-rationalization: How to cope with the design consequences
- c. Co-rationalization: a hybrid strategy to take parallel decisions affecting the rationalization of form together with the process of design.

The rationalization strategy was carried out by having a certain set of initial assumptions and rules as mentioned below;

- a. Maintaining a uniform gap between all six sides of the hexagon panel system
- b. Begin with a standard hexagon size dimension of 63cm diameter

- c. Scaling the hexagonal system from a diameter range of 63cm to 175cm
- d. Grouping the panels into different families which in turn reduces the number of unique panels for the fabrication/ production process

In addition to the above assumptions, it is stated that the other two major strategies considered in the pre-rationalization stage were

- (i) freeform space frame structure which acts as the panel positioning device and a supporting structure for aluminium panels and waterproofing panels and
- (ii) The Master Design Surface (MDS) was frozen as a fixed design component to avoid intermittent design and fabrication changes.

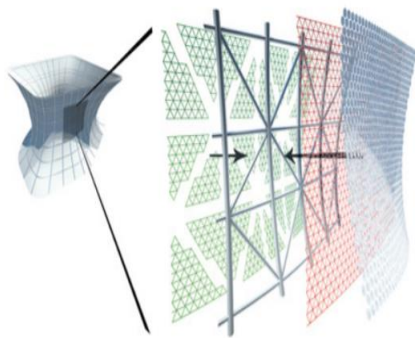


Figure 2.39: Layers during construction [28]



Figure 2.40: Layers considered [27]

It is stated that during the process, there were two rationalization strategies carried out to obtain the coordination data which were unsuccessful due to the type of complexity in the Master Design Surface (MDS).

- (i) The conformal and isometric mapping rationalization strategy for panelling the doubly curved surface was unsuccessful due to the reason that the surface was formed with NURBS (Non-Uniform Rational B-Splines) digitized from a physical model. It is stated that the wrapping of 2D drawings of panel layout over the complex NURBS surface preserved neither the length nor the angle, as conformal mapping is suitable only for the cylinder or a planar surface.
- (ii) The second rationalization strategy was the mapping of Gaussian Curvature properties onto the MDS. The mapping helps in obtaining areas on the surface with relatively low curvatures. Since this approach allows wrapping of 2D patterns on the complex surfaces, but it cannot provide the smooth transition between the areas of relatively high curvature differences.

Therefore, sphere packing or circle hex meshes rationalization strategy is stated to be considered to obtain the panel, strut and node assembly coordination data for manufacturing and assembly. The sphere packing rationalization strategy involves intersecting circles whose diameters have

the corresponding relation with the hexagon diameters. The circular mesh having intersecting circles with certain diameter were constructed having consideration for the actual diameters of the hexagon and the gap between the hexagons as shown in the Figure 2.41 and Figure 2.42.

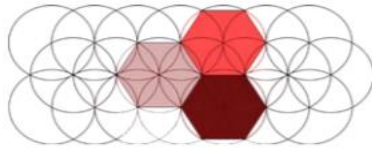


Figure 2.41: Hexagons enclosed by intersecting circles [21]



Figure 2.42: Hexagon diameter and gap [21]

From the circle mesh grid on the surface, the hexagonal patterns along with desired gaps are stated to be extracted. The other challenges involved was the correcting artefacts in the regions or areas with high curvature. Due to high curvature, the outer edges are stated to rise and retracted from the initial position due to a reduction in the height of the panels. The correction for the reduced height was carried out using the post-production process in which the initial step involved was the identification of all the panels that required corrections. Further, a curve was vertically passed through the points in the columns of panels starting from the top of the surface envelope and passing the boundary edge of the surface as shown in the Figure 2.43.

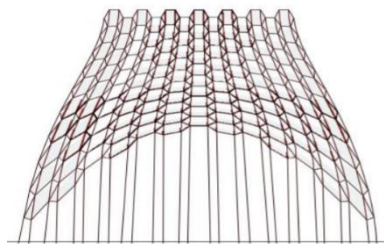


Figure 2.43: Vertical curves to stretch hexagons [21]

These curves are stated to be used as rails to pull the hexagonal panels down until the vertical and horizontal dimensions correspond to each other, i.e., the height to width ration on 60-degree hexagon was used to calculate the amount of percentage required to stretch the hexagon of the required height.

The below-mentioned Figure 2.44 represent the stretching of the hexagon on the complex shape.

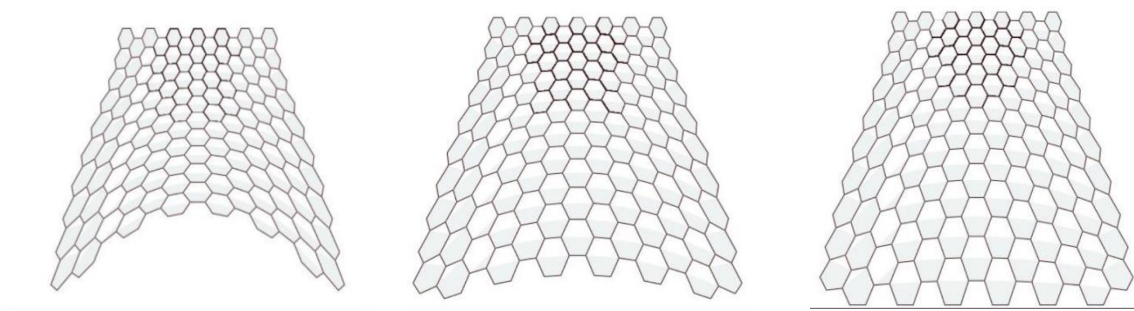


Figure 2.44: Stages in stretching [21]

The final stage of the design involved the reduction of the number of unique panels to avoid high manufacturing costs. It is stated that client asked for 7 or 24 unique type of panels all over the surface due to the fact of major challenges involved in a large number of unique panels, i.e., (i) cost of producing unique moulds for each, (ii) constructability challenges, and (iii) substructure frame design challenges. Therefore, a statistical approach of k-means clustering was carried out over the panel population by considering 21 parameters with the area of the panel being the key parameter. Thus, the designers were able to obtain the desired number of families with unique sizes. Figure 2.45 shows the final families of the panels obtained using the k-means clustering algorithm.



Figure 2.45: Final panel families [15]



Figure 2.46: Construction process [15]

Henceforth, it can be concluded that this case study gives a greater insight into the design challenges and solutions without compromising the aesthetics of the structure. The rationalization strategy of sphere packing, self-adjusting pattern stretching algorithm in parallel with k-means clustering for unique panel families gives the best solutions for the desired aspects.

There are plenty of important aspects such as the agent-based modelling technique to develop a pattern, structural analysis and interdisciplinary interactions related to data flow in case study 1 and panel grouping, panel relaxing etc. in case study 2 can be learnt. Based on those understandings, the optimization algorithm for the structurally stable free form structure formed by NURBS and panel distribution can be carried out. The next section represents the step by step procedure of the optimization algorithm.

3 Methodology for Optimization Process

There are two main objectives of this research work namely: (i) Optimization of freeform metal sheet assembled shell structure with respect to structural stability and (ii) Optimization of cell or panel distribution in full-scale sheet metal for an effective manufacturing process. The Rhino-Grasshopper platform provides numerous options to create a 3D surface based on the user's choice. In this research work, the number and type of components considered is based on the calculation time as the genetic algorithm experiences longer processing time.

3.1 Optimization of Shell Structure Form - Structural Stability

The methodology used for executing the former objective of the research work .i.e., the optimization process of shell structure assembled with metal panels, involves three important steps as mentioned below (see Figure 3.1);

- Creation of 3D shell surface having Voronoi pattern with different parameters.
- Basic structural analysis of the structure to obtain only the maximum displacement value.
- Application of genetic algorithm by using the value obtained in the 2nd step.

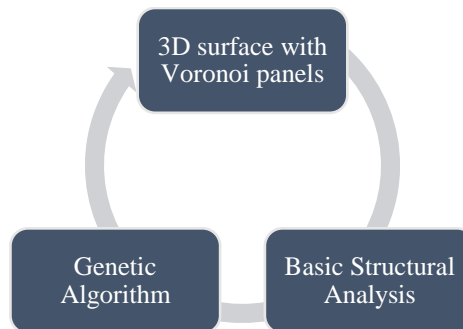


Figure 3.1: Optimization process for stable structure

So, with the above-mentioned steps, the study is carried out regarding the influence of Voronoi tessellations (either relaxed or irregular) on the structural stability together with the other parameters.

3.1.1 Creation of 3D Shell Surface with Voronoi Pattern

The 3D surface for the shell structure was created by using different components available on the grasshopper together with additional components from 3rd party plug-ins. The detailed description regarding the type of inputs fed and the outputs obtained from each component is mentioned in the following steps;

Step 1: Setting up a reference polygon to know the location of the shell structure

This step includes the creation of a reference polygon, which will give a basic idea of where the 3D surface should be created. This polygon is also used as a reference for the creation of ellipse at a certain height (description follows in further steps).

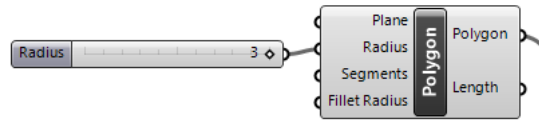


Figure 3.2: Polygon component in Grasshopper

Based on the input data required by each component, the following inputs are given to obtain the polygon as an output;

Table 3.1: Inputs for polygon component

Type of Input	Given input	Description
Plane	Plane XY	Polygon base Plane.
Radius	3	The radius of a polygon (distance from centre to tip).
Segments	11	Number of segments.
Fillet Radius	Default value = 0	Polygon Corner fillet radius.

Table 3.2: Outputs from polygon component

Type of Output	Output	Description
Polygon	Curve	Polygon.
Length	Number	Length of polygon curve.

The following output can be visualized in Rhino:

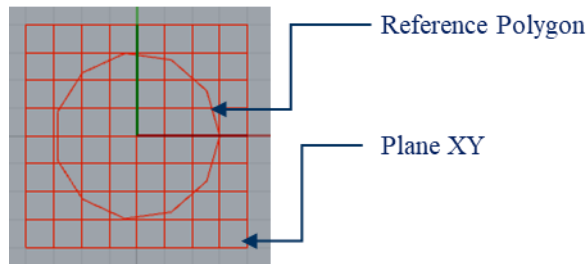
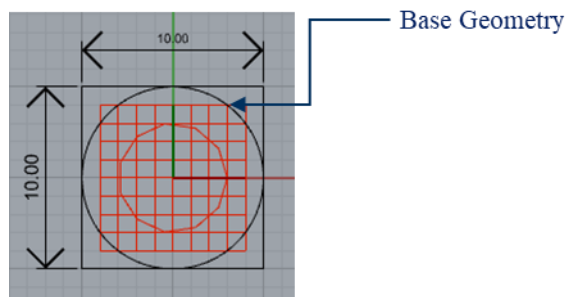


Figure 3.3: Reference plane and polygon

Step 2: Drawing a base geometry for the shell structure in Rhino

In this research, the base geometry for the shell surface is constrained between 10m x 10m square (can be user’s choice). The geometry is drawn in Rhino.



Step 3: Setting up an ellipse at a certain height from the base geometry to maintain the height of the shell structure

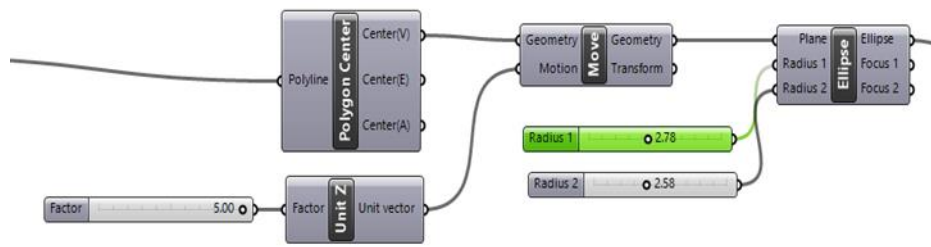


Figure 3.4: Creating an Ellipse at certain height

- The centre of the set polygon on plane XY is extracted
- It is moved to a certain height using a vector in the z-direction (height can be varied between 3.00m to 5.00m).
- This moved point acts as a plane for the ellipse
- The radii of the ellipse are defined

Table 3.3: Inputs for Ellipse component

Type of Input	Given input	Description
Plane	Plane at a point	Base plane of the ellipse.
Radius 1	1.00 to 5.00	Radius in {x} direction.
Radius 2	1.00 to 5.00	Radius in {y} direction.

Table 3.4: Output from Ellipse component

Type of Output	Output	Description
Ellipse	Elliptical Curve	Resulting ellipse.
Focus 1	Co-ordinates of Point 1	First focus point.
Focus 2	Co-ordinates of Point 2	Second focus point

The following output can be visualized in Rhino:

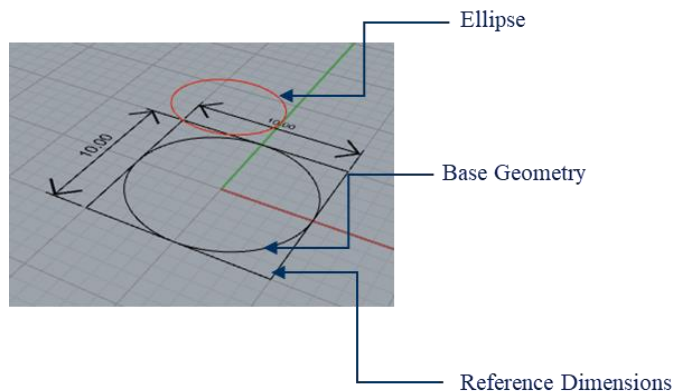


Figure 3.5: Visualization of Ellipse in Rhino

Step 4: Dividing the top ellipse and bottom base geometry into several segments to obtain many points.

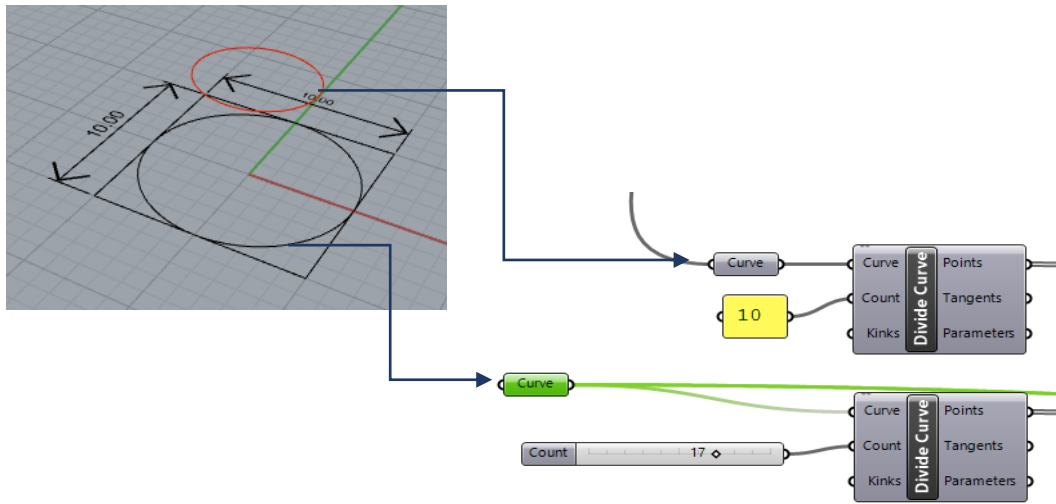


Figure 3.6: Process for geometry division

- The base geometry and top ellipse are divided into several segments to obtain the list of points.
- For an ellipse, the number of counts considered is between 3 and 10 (user’s choice).
- For base geometry, the number of counts considered is between 10 and 20 (user’s choice).

Table 3.5: Input for Ellipse Segmentation

Type of Input	Given input	Description
Curve	Ellipse	Curve to divide.
Count	3 to 10	Number of segments
Kinks	False	Split segments at kinks

Table 3.6: Input for Base Geometry Segmentation

Type of Input	Given input	Description
curve	Base Geometry	Curve to divide.
count	10 to 20	Number of segments
kinks	False	Split segments at kinks

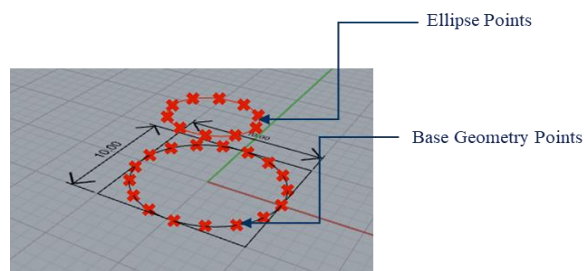


Figure 3.7: Output after division of geometry

Figure 3.7 shows the obtained output after dividing the top and bottom geometry into several segments and all points of each segment are necessary to proceed with the next steps.

Step 5: Picking a single point from the ellipse and inserting into the list of points of base geometry.

The point list generated by the divide curve component for ellipse and the base geometry is carefully visualized. For example, point 3 of an ellipse is inserted into the point list of bottom base geometry at 1st and 6th position. The selection of the point and insertion places are free to be chosen by the user. Thus, there are no restrictions on choosing a particular point. If the chosen point is inserted at tow positions, then the structure has two openings. Therefore, the number of places the point is inserted into the list defines the number of openings.

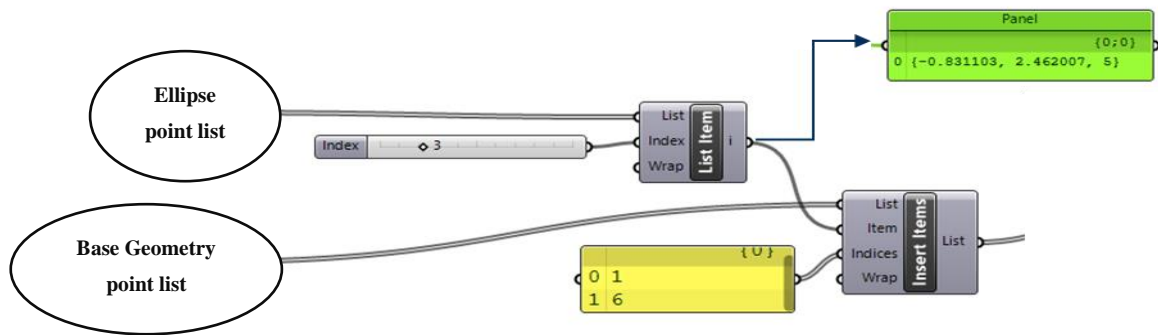
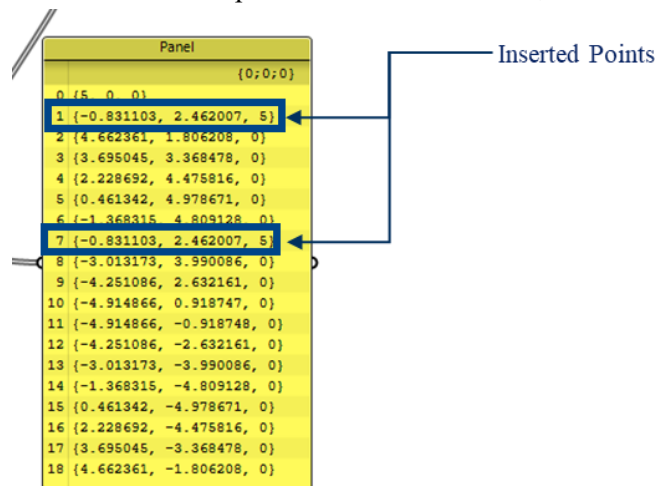


Figure 3.8: Creating a list of points for NURBS curve

The slider in Figure 3.8 represents the chosen point in the ellipse point list and the grasshopper component “list item” allows the user to choose a particular item in the list. It can be very well seen that the panel has co-ordinates of point 3 of an ellipse. This point co-ordinate is plugged into the user-defined positions in the point list of the base geometry using the grasshopper component “Insert items”.

The final output of the “Insert item” component can be seen below;



Step 6: Creating a NURBS curve with the point list created in previous step

The point list created in step 5 is inserted as an input for the “NURBS Curve” component. Based on the theoretical explanation mentioned on NURBS curve in the section 2.3, the inputs are given as mentioned in Table 3.7 and Figure 3.9 shows the obtained output in the form of Rhino visualization.

Table 3.7: Inputs for NURBS curve component

Type of Input	Given input	Description
Vertices	List created	Curve control points
Degree	3	Curve degree
Periodic	True	Periodic curve

Table 3.8: Output from NURBS Component

Type of Output	Output	Description
Curve	NURBS Curve	Resulting NURBS curve.
Length	Number	Curve length.
Domain	Domain	Curve domain.

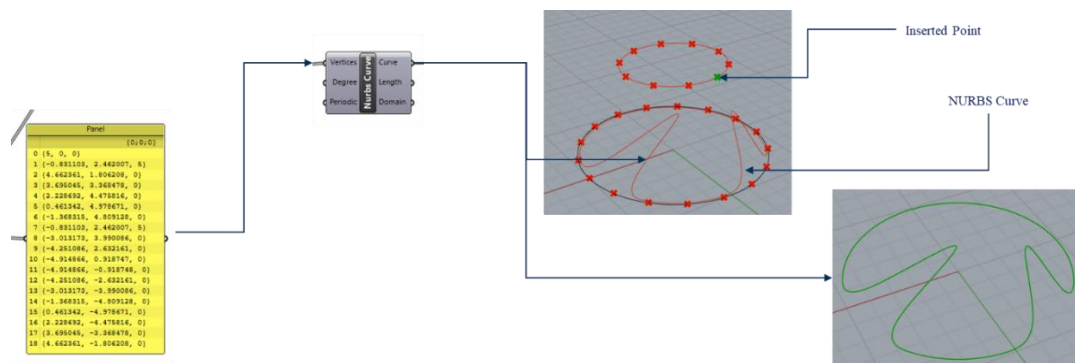


Figure 3.9: Rhino visualization of NURBS curve

Step 7: Creating a surface from the generated NURBS Curve

The “patch” component in the grasshopper gives the user to create an incredible free form three dimensional patch surface, which can be controlled by the control points of the NURBS curve. Table 3.9 represents the inputs given and Figure 3.10 shows the output of the patch surface.

Table 3.9: Inputs for Patch component

Type of Input	Given input	Description
Curves	NURBS Curve	Curves to patch
Points	0	Points to patch
Spans	10	Number of spans
Flexibility	1	Patch flexibility (low number; less flexibility)
Trim	True	Attempt to trim the result

Table 3.10: Output from Patch component

Type of Output	Output	Description
Patch	Surface	Patch Result.

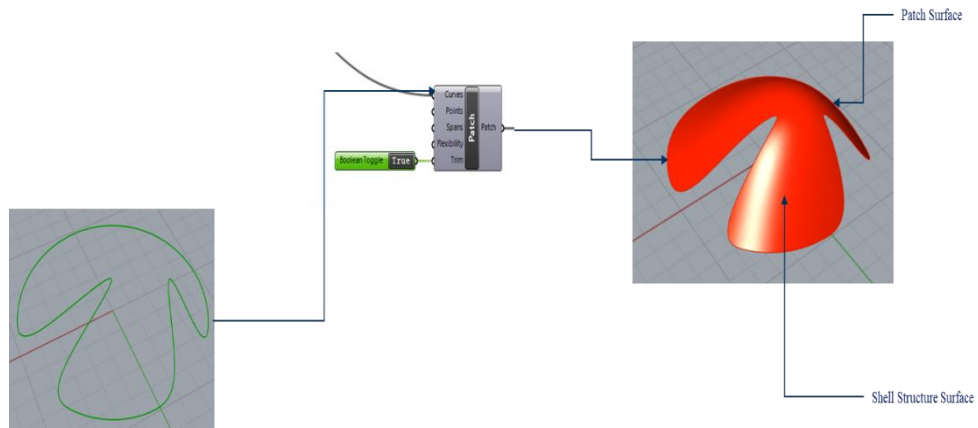


Figure 3.10: Rhino visualization for Patch surface

Step 8: Creating Voronoi tessellation on 2D Surface

To create a Voronoi tessellation, it foremost required to have a set of randomly distributed points as mentioned in section 2.4. Although grasshopper has a 3D Voronoi tessellation component, it was not used in this research due to the fact of higher computation time and also, 2D Voronoi tessellation serves the same purpose as 3D Voronoi tessellation for this research study. Thus, the latter enabling lower computation time in comparison with the former.

The points are randomly generated on the 2D surface within the chosen shape of the base geometry using the component “populate geometry.” The 2D Voronoi tessellation is generated by using the output of “Populate geometry” as an input to the “Voronoi” component. Figure 3.11 below along with Table 3.11, Table 3.12, Table 3.13 and explains the state of inputs and the outputs obtained in the form of Rhino visualization. It shall be noted that the boundary of Voronoi tessellation 2D surface is within the approximated rectangular boundary with respect to the given base geometry (it differs for the negative curvatures and polygons).

Table 3.11: Inputs for Population component

Type of Input	Given input	Description
Geometry	Rectangular surface generated from given base geometry	Geometry to populate (curves, surface, breps and meshes only)
Count	210 (randomly chosen number)	Number of points to add
Seed	1	Random seed for insertion
Points	Empty	Optional pre-existing population

Table 3.12: Outputs from Population component

Type of Output	Output	Description
Population	Points	The population of inserted points

Table 3.13: Inputs for Voronoi component

Type of Input	Given input	Description
Points	Rectangular surface generated from given base geometry	Points for Voronoi diagram
Radius	Empty	Optional cell radius
Boundary	Base geometry	Optional containment boundary for diagram
Plane	Empty	Optional base plane.

Table 3.14: Output from Voronoi component

Type of Output	Output	Description
Cells	Points	Cells of the Voronoi diagram

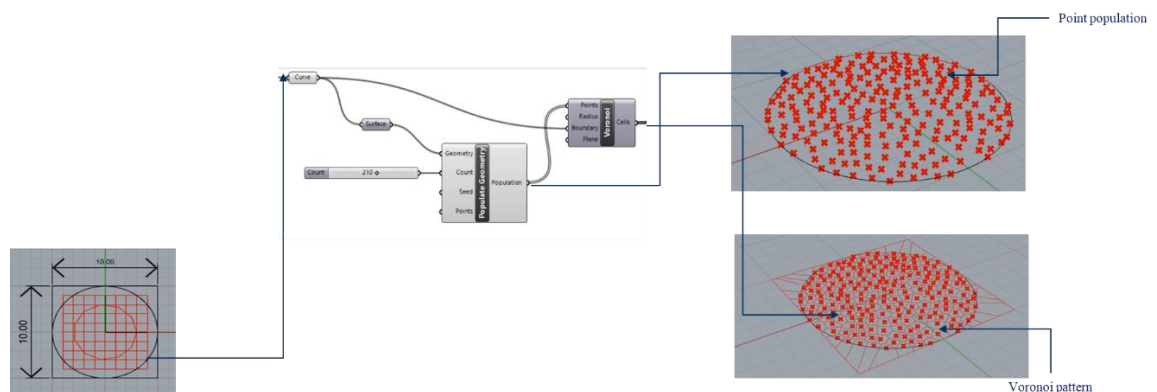


Figure 3.11: Voronoi visualization in Rhino

Step 9: Trimming the Voronoi pattern on a 2D plane to the required surface area

Since it is mentioned in the previous step that the Voronoi tessellation is generated for the rectangular boundary with respect to the given base geometry, it is therefore needed to trim out the irrelevant set of Voronoi cells outside the base geometry. Hence, the grasshopper component “Trim with Region” is utilized to serve the purpose.

The set of inputs for “Trim with Region” is shown in the Figure 3.12 and the procedure is as explained below;

- The generated NURBS Curve is projected onto the 2D surface using the component “Project Geometry”. The output of this particular component is used as a “Region” input for the first component “Trim with Region”, while the “Curve” input receives the Voronoi cells.

- In the other “Trim with Region” component, the “Region” input takes Voronoi cells and “Curve” input takes the NURBS Curve.
- The output of these two “Trim with Regions” components represented as “Inside” is subjected to cleaning using the “Clean Tree” to remove the Null values in the list of curves.
- Then, the list of curves are joined to act as one unit using the component “Join Curves” (see Figure 3.12).

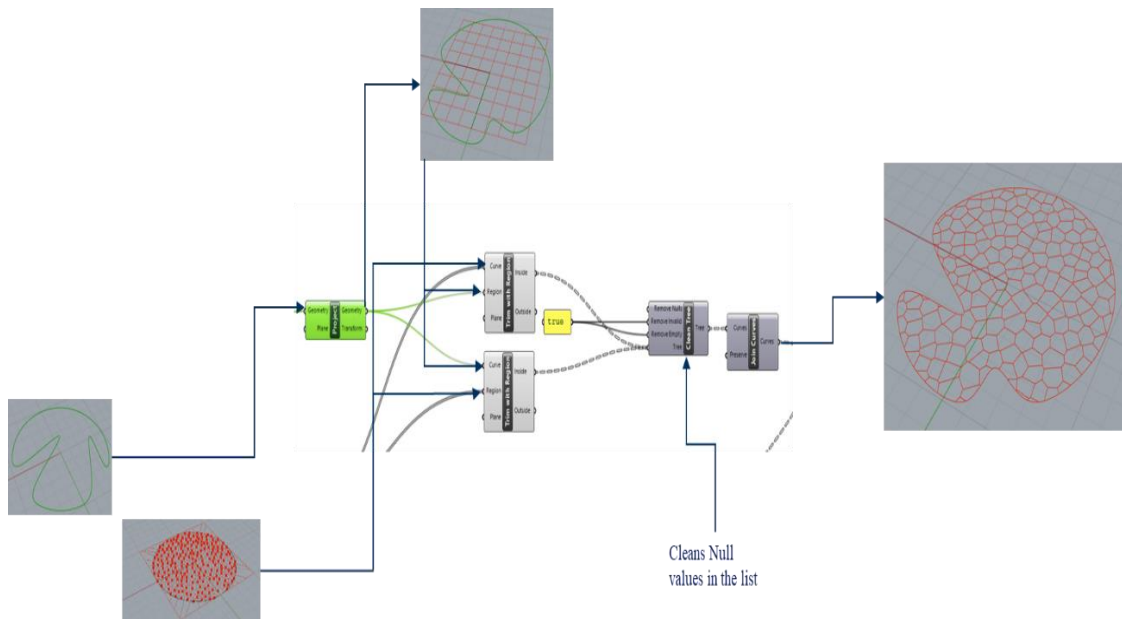


Figure 3.12: Trimming the regions of Voronoi

Step 10: Projecting the trimmed Voronoi pattern onto the shell surface and reducing the curvature of cells to the tolerance value

Since the Voronoi tessellation has been developed in the previous step, the main aim is to obtain the Voronoi tessellation onto the shell surface created in step 7. The grasshopper component which is suitable for the defined aim is the “Project”. The “curve” and the “Brep” inputs for the component gets the trimmed Voronoi 2D tessellation and the shell surface respectively. Figure 3.13 show the complete detail about this step. In addition, as the curvature has certain slopes and this was reduced by fixing the corners of the Voronoi tessellation at the same points as projected and curves were replaced by the polyline joining the corner. This step was carried out using the “Curve to Polyline” component.

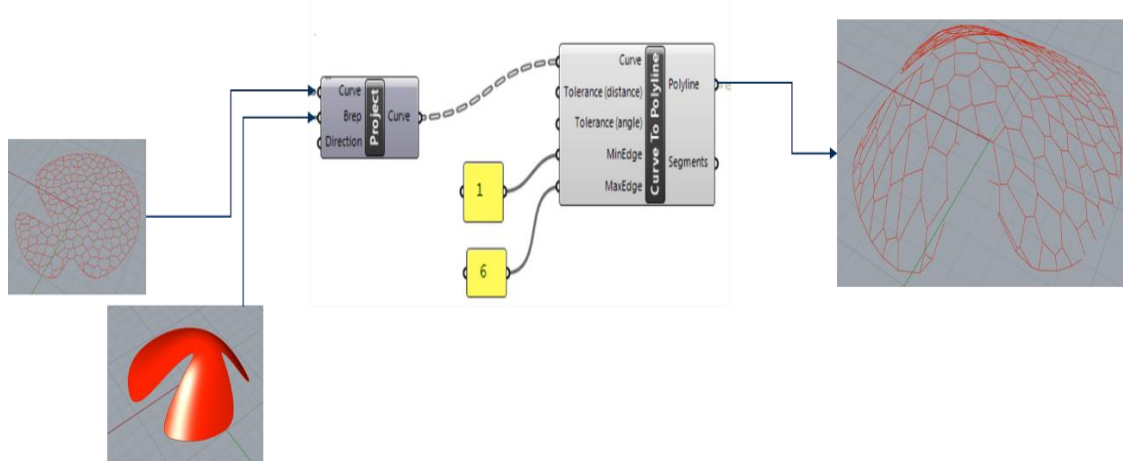


Figure 3.13: Projecting Voronoi panels with reduction in curvature

Step 11: Closing the naked or open edges of cells to closed edges using a component from Weaverbird

In the previous step, it can be noticed that the generated Voronoi tessellation shell surface has open edges and this issue can be resolved using a 3rd party plug-in for Rhino generated by Weaverbird as “Weaverbird’s Naked Boundary” component. The generated polylines in step 10 serve as an input for this component and the generated output can be visualized in the Figure 3.14.

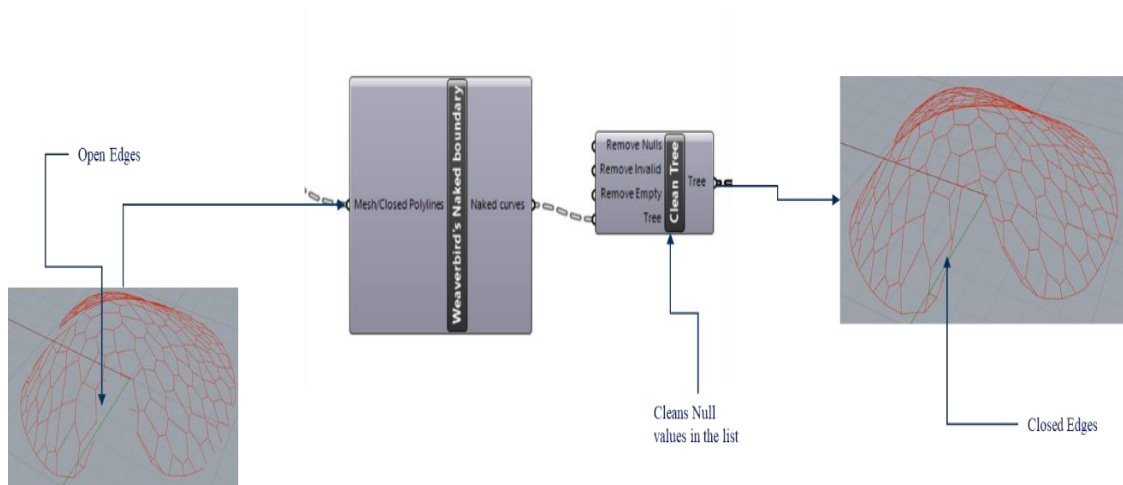


Figure 3.14: Closing naked edges

Step 12: Measuring the dimensions of the edges.

This step is not an essential part of this research work. However, the dimension of the edges can be used for visualization for further steps such as during the relaxation process of Voronoi tessellation. The procedure to determine the dimensions of the edges is as shown in the Figure 3.15 .

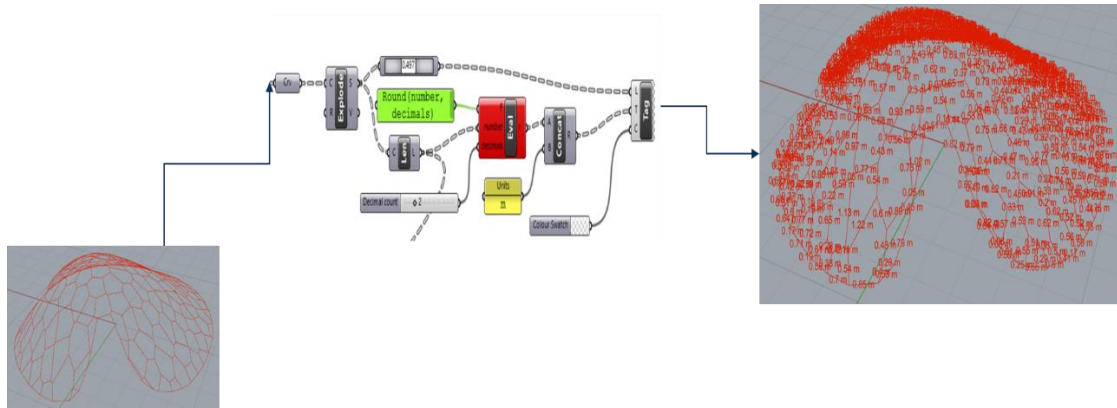


Figure 3.15: Dimensions of panels on the shell structure

In the process of measuring the dimensions of the edges, the generated closed edge curves serve as input and it is exploded to form individual elements in the list. Then, the length of the curve is calculated using the “Length” component. The value obtained is then approximated with two decimal values and concatenated with the term “m” which defines meter. Finally, the values are tagged to the curves using the component “tag.”

Step 13: Setting offset of edges to have a clear picture of cells

This is considered only to be a visualization step, which shows the clear shapes of each panel. The components used in this step involves “Polygon centre”, “Scale” and “Custom Preview.” Figure 3.16 represents the clear visualization of panels in Rhino.

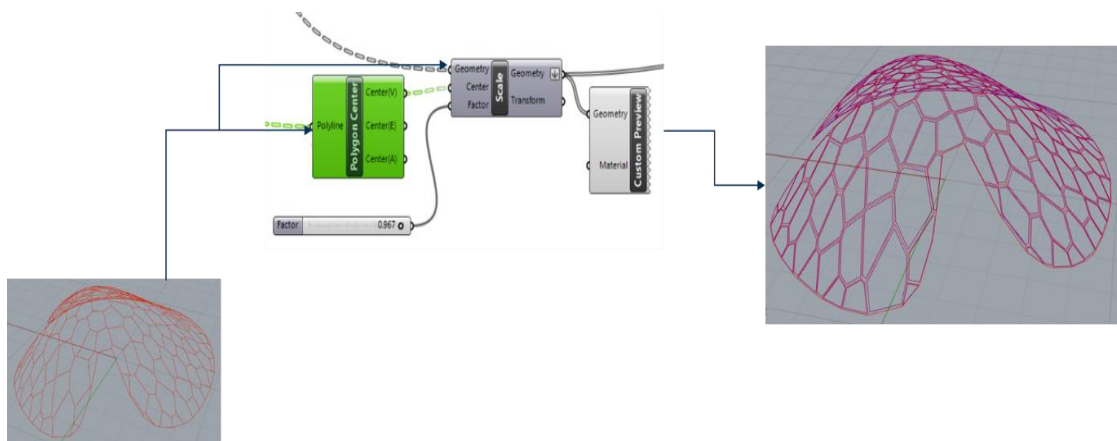


Figure 3.16: Setting offset of edges

Step 14: Proportionating / Relaxing Voronoi cells using Lloyd’s algorithm

Based on the section 2.4.5, Lloyd’s algorithm is implemented using the 3rd party plug-in known as “Hoop Snake.” This component gives freedom for the user to start and end the iteration along with the feature of automatic iteration process with the termination condition. The components are set in the following order as shown in the Figure 3.17. The “Populate Geometry” component serves as input for the starting data. The output in the form of “Feedback” is connected to the “Voronoi” component. The centroidal points of these Voronoi cells are calculated using the

“Area” component. These centroidal points are allowed to shift by connecting the output of “Area” component to the data of Hoop snake. Thus, with this process, the Voronoi relaxation technique is achieved (see Figure 3.17).

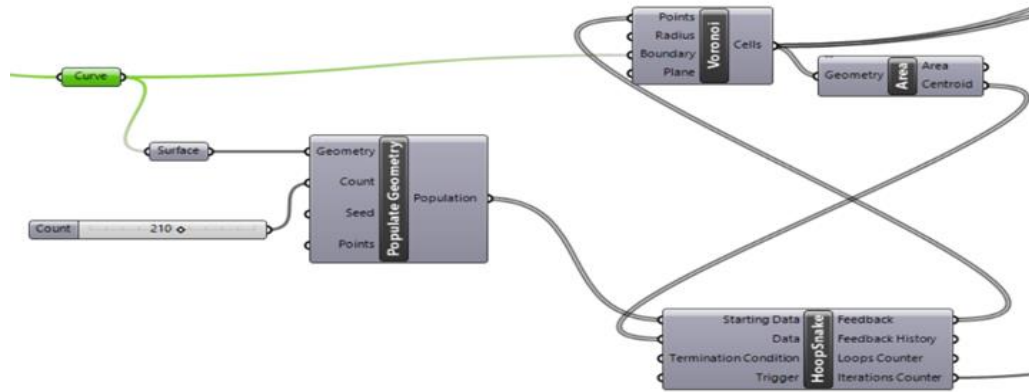


Figure 3.17: Algorithm for Voronoi relaxation

Based on the above-mentioned algorithm, the following output (see Figure 3.18) is obtained which represents the Voronoi pattern after relaxation. The panels can be seen as proportional to each other and are as desired. It shall be noted that the surface for the panels is created using the component from Weaverbird known as “Weaverbird’s Catmull-Clark Subdivision.”

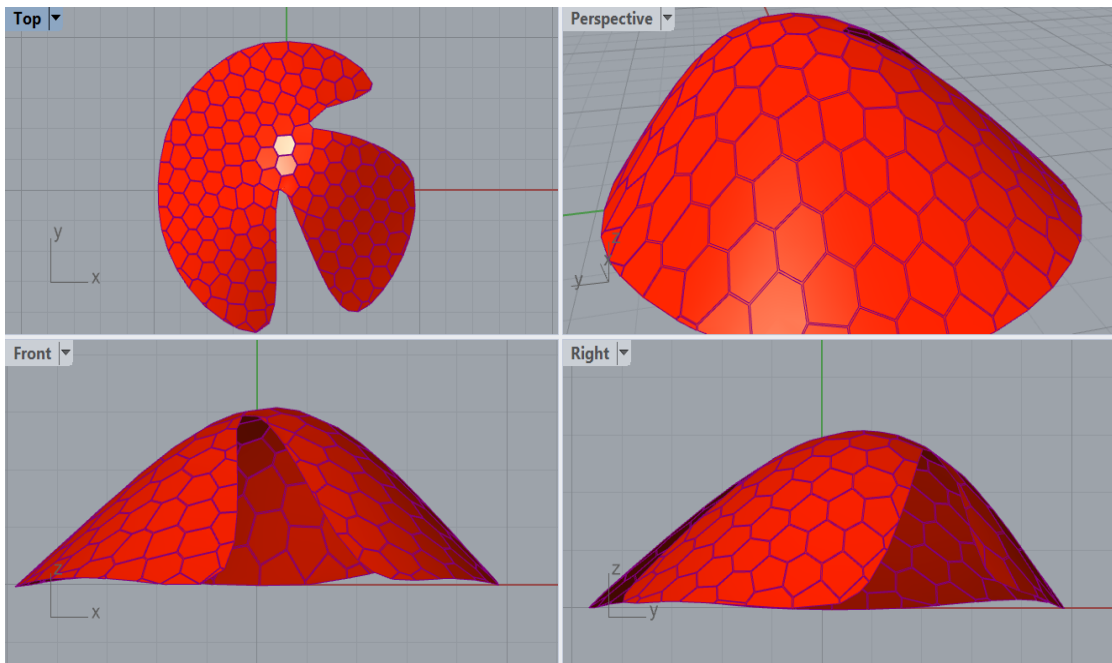


Figure 3.18: Relaxed Voronoi pattern-Rhino

Step 15: Check for flatness and obtaining centre of gravity of panels

Although, the Grasshopper provides a component that features check for panel flatness as a whole, it was not suitable to the process flow of this research algorithm due to the absence of planar surface. Hence, a component known as “Planar” is used to check the planarity of the polygon curves forming each panel. The output of the component signifies that those polygon curves having a value ‘0’ is perfectly planar or flat (see Figure 3.19). However, it was noticed very few polygon curves has a value ‘0’. But, the other deviation values in the list also signifies that the polygon curves with deviations close to zero represents the curves near to flat. Hence, it is assumed that all the panels are close to flatness and shall be considered for further study process. Figure 3.20 shows the centre of gravity of each panel and panel numbering.

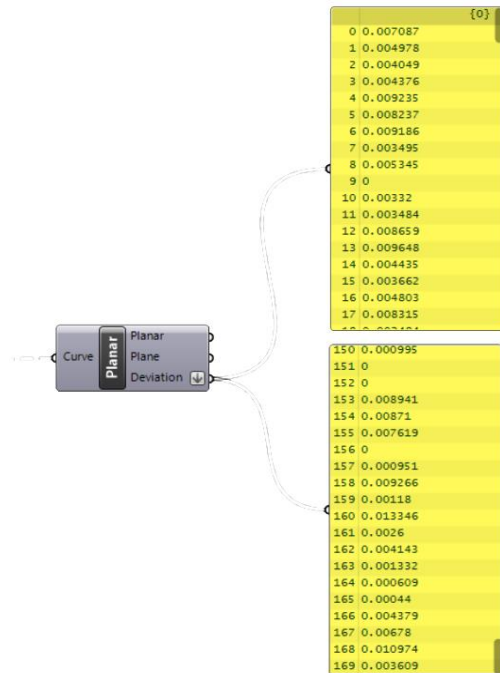


Figure 3.19: Flatness check

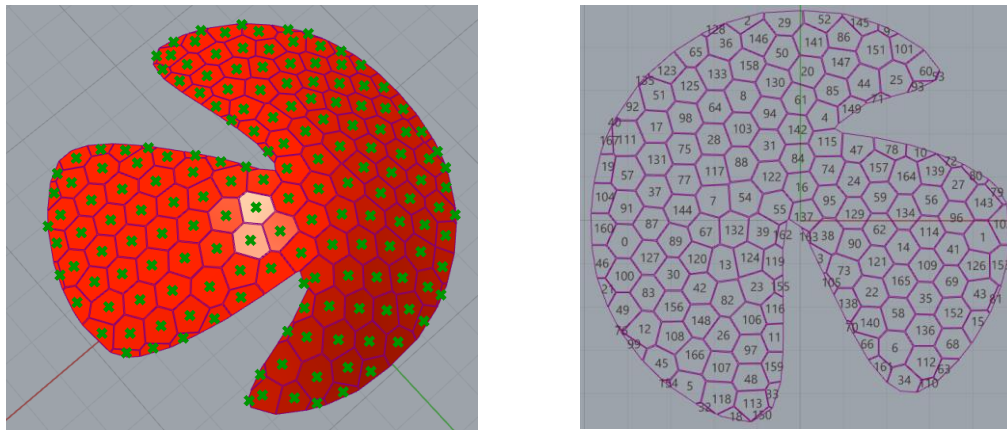


Figure 3.20: Centre of gravity of each panel and panel numbering (Top View)

The above mentioned steps does represents the work flow of the algorithm. But, the figures representing the form of the structure is not the final the form (see Appendix A4 for alternate forms). Therefore in order to obtain the structurally stable form, there is a need to perform a basic structural analysis which delivers a reference value known as the fitness value for genetic algorithm.

3.1.2 Basic Structural Analysis for Fitness Value

As the research work is directed towards the form of the shell structure based on structural stability, it is therefore required to perform certain basic structural analysis. Because, the genetic algorithm is certainly dependent on a fitness value and performing structural analysis directs the research work towards this value. The structural analysis is performed on a grasshopper plug-in known as Karamaba 3D. In depth structural analysis was not a scope of work in this research. Therefore, basic assumptions are considered while performing the structural analysis and are as described below;

- The sheet panels are assumed to have beam like connection, instead of performing analysis for the sheet as a whole, i.e., the joint between the panels is assumed as a beam of rectangular steel section (For further details, see material assignment section)
- The structural analysis is performed using the first-order theory of small deflections.
- Only gravity load and self-weight are considered.
- The joint between the elements is considered to have hinges.

The detailed description regarding the type of inputs fed and the outputs obtained from each component is mentioned in the following steps (Steps are continued from the previous section);

Step 16: Converting the polyline curves into beam elements

The component “Weaverbird’s Naked Boundary” + “Clean Tree” produces an output in the form of polygon curve representing Voronoi cells (see step 11). These polyline curves or line-like curves are converted into single straight elements using the combination of “Explode” and “Line to Beam (Karamba3D)” components (see Figure 3.21).

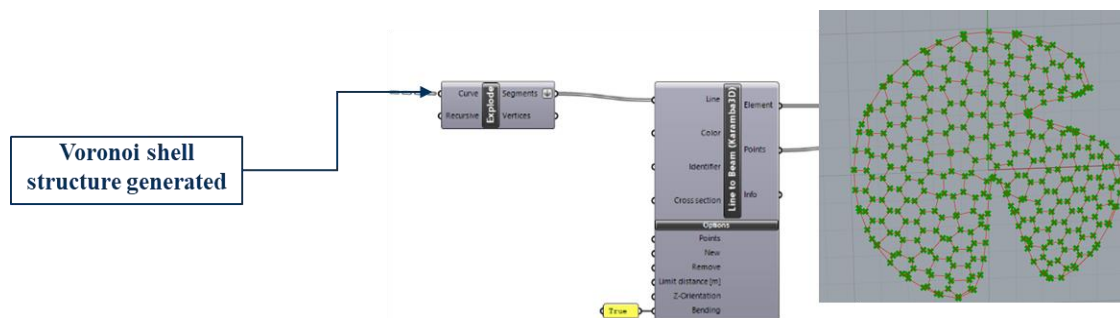


Figure 3.21: Line to Beam

Step 17: Defining loads

The Karamba 3D plug-in permits various ways of assigning loads to the structure and in this case simplest of all the ways is considered. From Figure 3.22, it can be seen that the gravity load and self-weight in the form of point load are applied to the nodes of the Voronoi cell pattern. The inputs and outputs of the components are well defined.

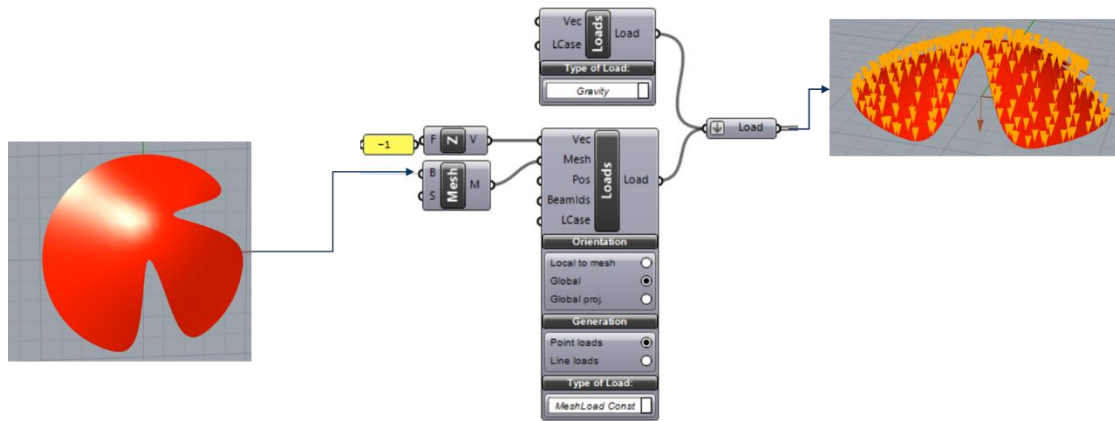


Figure 3.22: Defining loads

Step 18: Defining joints, material and cross-section

The component considered to define the joints is “Joint-Agent” and it is defined as a hinged joint by choosing rotations in x, y, and z directions (see Figure 3.23). The materials and section defined are steel and rectangular section respectively (see Figure 3.24).

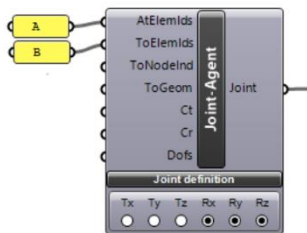


Figure 3.23: Defining Joint

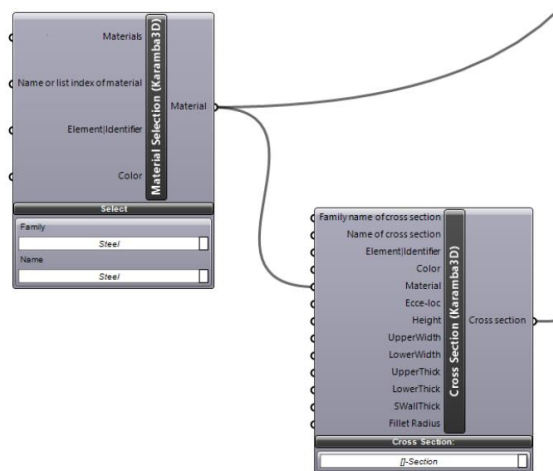


Figure 3.24: Defining material and cross-section

Step 19: Defining support conditions

The support conditions can be differently set up, i.e., fixed end supports or hinged support etc (see Figure 3.25). The points of the supports are obtained by using the list of points obtained from the “Line to Beam (Karamba 3D)” component and points with lowest level in z direction are considered, i.e., the selection of points is carried out by visualization in Rhino.

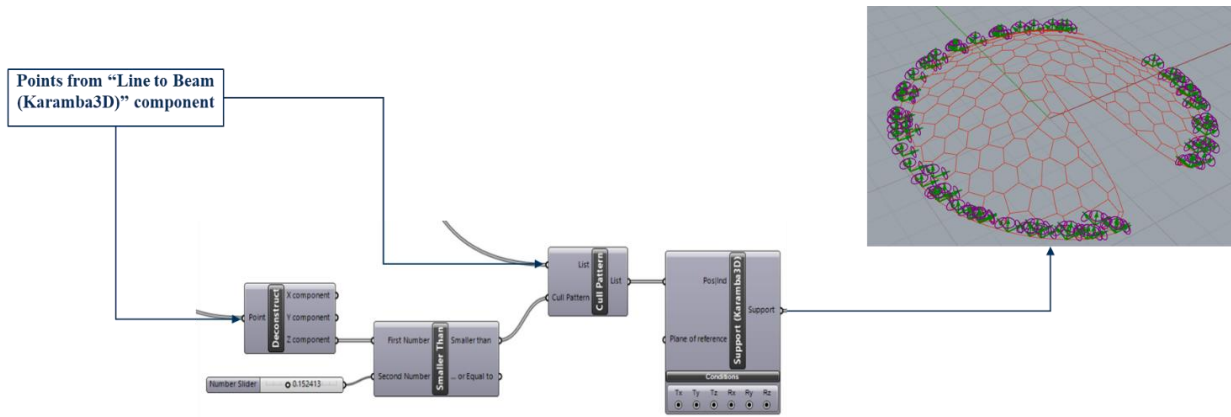


Figure 3.25: Defining supports

Step 20: Model Assembly and analysis

All the above-mentioned conditions or criterion are assembled together using the “Assemble Model (Karamba 3D)” component (see Figure 3.26). Then the whole model is subjected to structural analysis using first order theory for small deflections in-order to obtain the “maximum displacements [cm] of each load-case of the model at end-points and mid-points of elements “is considered as a fitness value.

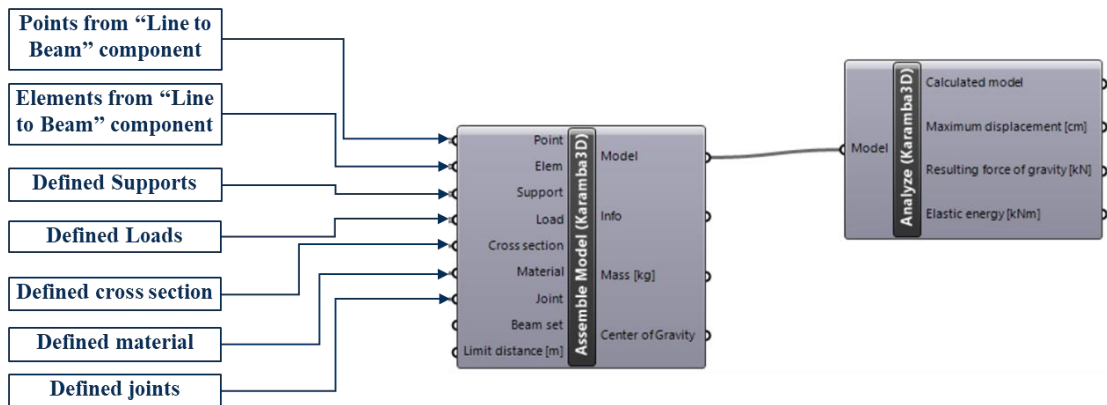


Figure 3.26: Model assembly and analysis

Step 21: Components to visualize the analysed results

Below mentioned are some of the components that are helpful to visualize the results in the form of numbers along with different colours (see Figure 3.27). In order to view the results of stresses, shear forces in elements and support reactions refer to Appendix A1.

- Beam Resultant Forces – gives normal force, resulting bending moment and shear forces
- Beam Forces – gives normal force, shear force in y and z directions, torsional bending moment, and bending moments in y and z directions.
- Reaction forces - gives reaction forces and moments, support position, the sum of reaction forces and moments.

- Nodal Displacements – Nodal translations and rotations
- Modal View and Beam View

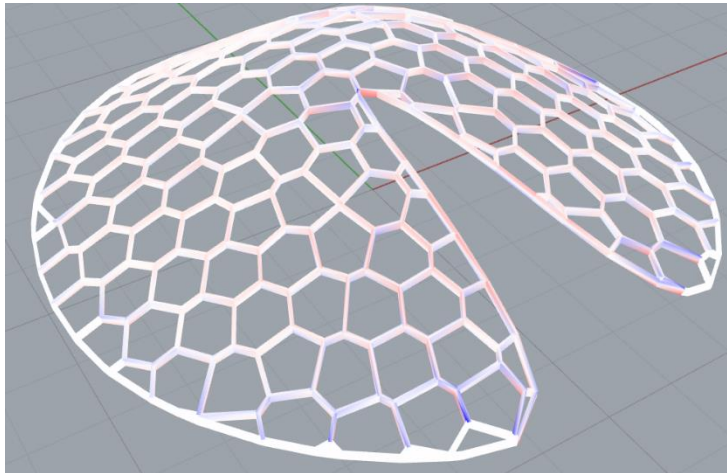


Figure 3.27: Visualization of stress distribution in the model

The optimization process for obtaining the stable free form structure is carried out by connecting various parameters to the genetic algorithm-Galapagos based on the fitness value obtained as “maximum displacement.” Hence, Results and Discussion section explains in detail about the parameters considered for various cases.

3.2 Optimization of Cell or Panel Packing

The second aim of this research work is to optimize the panel distribution in a full-size metal sheet, whose data can be further extracted and utilized for metal sheet manufacturing process such as the laser cutting. The optimization process is carried out to have a designated pattern or distribution of cells in the full size metal sheet to avoid material wastages during the manufacturing process.

Although the optimization process is also carried out using Genetic algorithm, there are certain limitations with which the research work has been performed at this particular stage. Some of the limitations or major challenges restrained this research to go in depth for the distribution of panels are as mentioned below:

- The panels that form a 3D shell structure have a minor deviation in the flatness and this deviation is certainly accepted by the industry. However, the Grasshopper do not allow these unflattened panels to be unrolled on a 2D plane. Hence, the panels are projected onto a 2D plane which allows to move ahead for further steps in the optimization process. Besides, the data is extracted from the optimized 3D shell surface (see section 3.1.1), there are slight variations in the panel sizes considered in nesting or packing process.
- It is well known that the panel shapes does not resemble the actual assembly of the 3D shell surface, i.e., no exact panel shapes with bend region and cut outs are considered (as shown in this research work[22]).

Although there are certain limitations, this generated optimization algorithm can be applied to any 3D shell structure with random base geometry and flat panel shapes. If the above mentioned limitations or challenges are resolved, this algorithm can be applicable.

Optimization process using genetic algorithm goes on with the following steps;

Step 1: Extracting fourteen random cells or panels from the optimized 3D shell structure.

In this step, the fourteen (random number- user's choice) different randomly picked panels from optimized 3D shell structure is extracted. The extraction is carried out by using a component "Random Reduce." The input has the list of polyline curves representing Voronoi cells of the optimized 3D shell structure and the output has the list of randomly picked cells (see Figure 3.28).

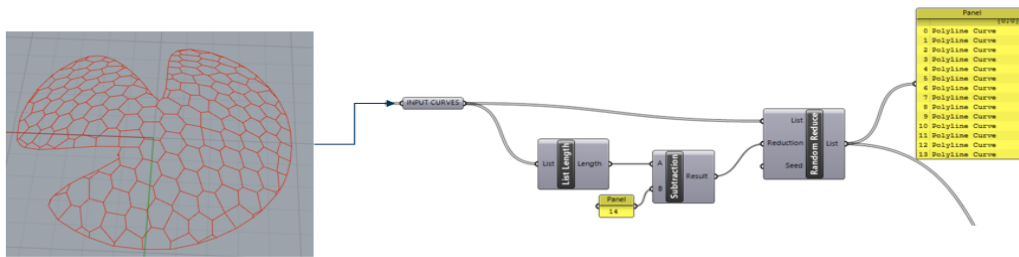


Figure 3.28: Random picking of Voronoi cells for nesting

Step 2: Generation of random points for the centroids of the panels

In this step, random points are generated using two gene pool of grasshopper. The two gene pool (pink boxes) represent co-ordinates for x-axis and y-axis of points. The gene pool takes the input as mentioned in the "GeneList Editor" (see Figure 3.29). The inputs for this editor is user dependent and in this research work, a square sheet with dimensions 15m x 15m is considered. Hence, the maximum value in the editor is mentioned as 15. (Note: These dimensions are only considered for demonstration purposes). The actual full size metal sheet available in the market have a dimension of 2m x 6m.

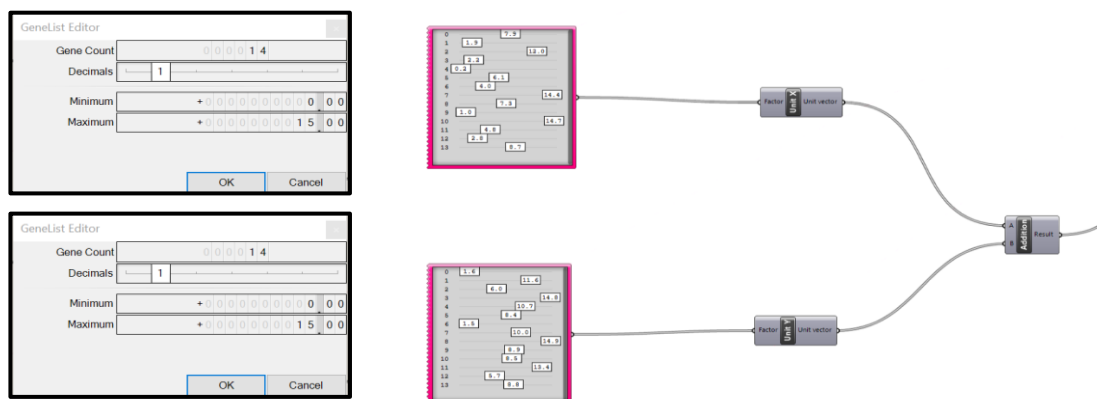


Figure 3.29: Generation of random points and sheet

$$fitness\ value = (Area * 0.5) + result \quad (Eq. 15)$$

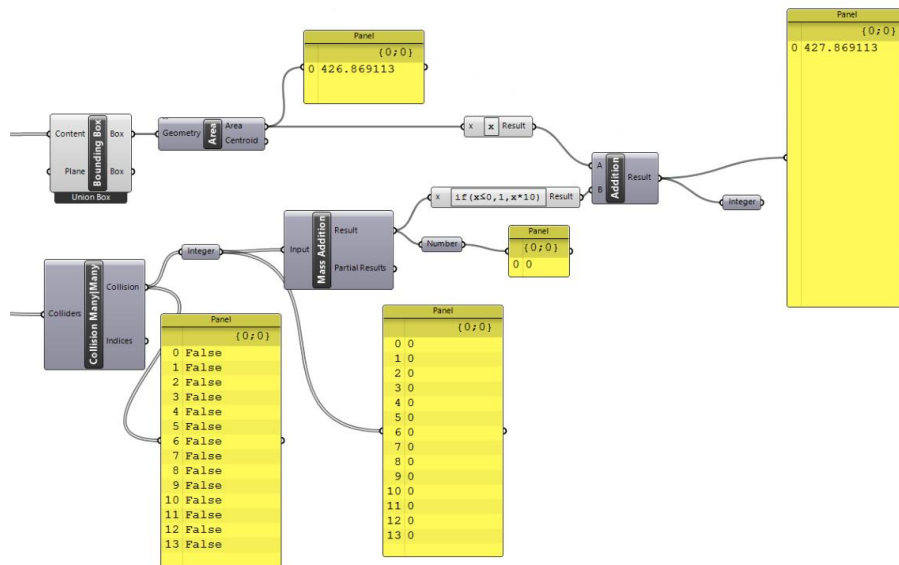


Figure 3.31: Collision check and fitness value generation

Step 5: Measuring the dimensions of the panels on the sheet

The method was also applied during the measurement of panels in the optimized shell structure in the previous task. The aim of the step (see Figure 3.32) to gather data for dimensions which can be further utilized for refining the laser cutting operations.

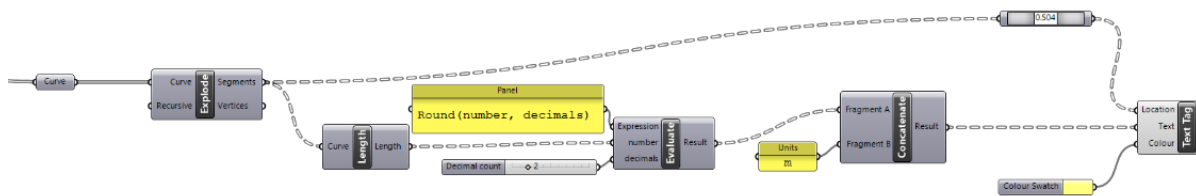


Figure 3.32: Measuring dimensions of panels on 2D sheet

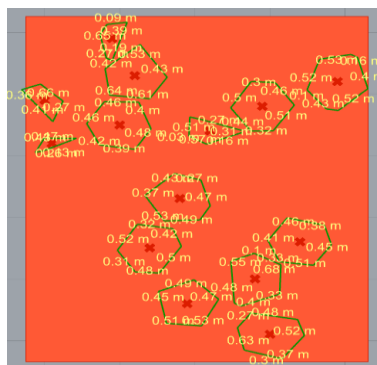


Figure 3.33: Visualization of dimensions (Not optimized)

Step 6: Measuring the internal angular dimensions of the panels on the sheet

The internal angles of the panels are measured using basic mathematical rules of radians. The method used for generating the angle on the 2D sheet is as shown in the Figure 3.34. The appearance of the output on Rhino is shown in the Figure 3.35.

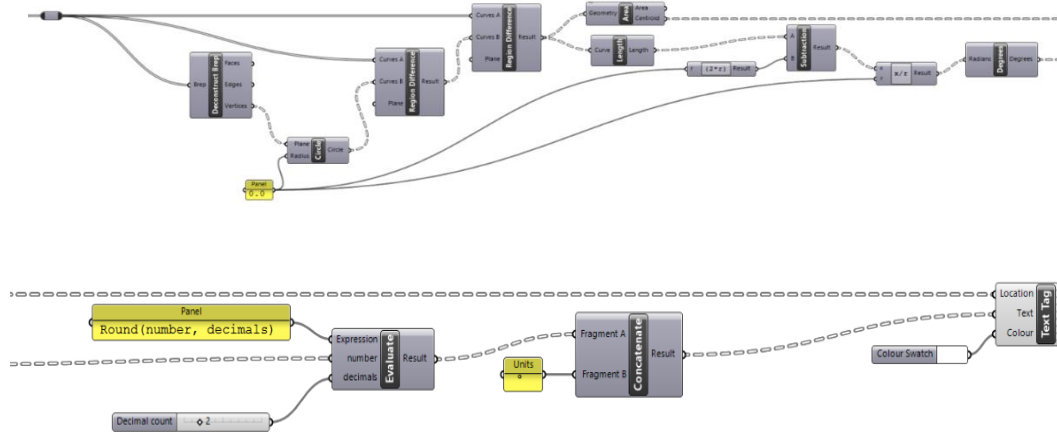


Figure 3.34: Internal angular measurement

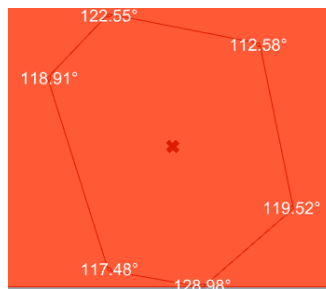


Figure 3.35: Visualization of internal angles

Now, the panel distribution or nesting is ready to be optimized by running a built-in genetic algorithm component of Grasshopper known as the “Galapagos”. The results are generated by connecting the Galapagos component to different parameters or gene pool. Optimization process and connection of gene pools for individual cases are discussed in the Results and Discussion section.

4 Results and Discussion

4.1 Optimization of Shell Structure Form - Structural Stability

With reference to the grasshopper algorithm developed in the section 3.1.1 and section 3.1.2, the optimization process to attain a structurally stable free form metal sheet shell structure is carried out by connecting a component known “Galapagos” (see Figure 4.1) The following results are demonstrated for various cases in order to show the efficiency of genetic algorithm for any suitable application.



Figure 4.1: Galapagos component in Grasshopper

4.1.1 Case 1: Form with Single Opening and Irregular Voronoi Tessellation

Aim: To obtain the form of the structure with a single opening, which results in minimum displacements.

Inputs: Table 4.1 defines the various types of parameters with which a shell structure attains a shape. The parameters include the width and height of the base geometry (circular), number of Voronoi panels and its dimensions set between a certain range based on visualization. The single opening of the structure is obtained by inserting a point of the upper geometry at position 1 of the NURBS list. Table 4.2 defines the inputs for genetic algorithm. However, the number of individuals in each generation is set to 20 with an initial boost of 40 and a maximum number of stagnant generations before the algorithm aborts are set to 50 and fitness value is subjected to minimization.

Table 4.1: Geometrical inputs for Case 1

Preliminary set up	Value	Description
Base Width	10 m	User's choice
Base Length	10 m	User's choice
Voronoi cells	210	User's choice
Lloyd's iteration	0	User's choice
Approximate range for length of each side of panel	0.2 m to 0.8 m	Depends on number of Voronoi cells and relaxation (visual check)

Table 4.2: Inputs for Genetic algorithm of Case 1 (Galapagos)

Gene Pool	Form	Range set	Type of value	Influence
Height	Number slider	3.00 to 5.00	Real (two decimals)	Structure height
Division in base geometry	Number slider	10 to 20	Integer	Structure shape
The point in upper geometry	Number slider	1 to 10	Integer	Structure shape

Outputs: After running the genetic algorithm, the following outputs are attained defining the lowest fitness value, i.e., maximum displacement has the lowest value of all the generations (see Figure 4.2). The shell structure with the lowest displacement can be seen with colour codes signifying low axial stresses (Figure 4.3 and Appendix A3).

- Height of the structure = 3.21 m
- Division in base geometry = 20 divisions
- A point in the upper geometry = 10th point
- Fitness value or Maximum displacement = 0.114068 cm
- Number of iterations / combinations checked = 2561

The following graphs represent the values of the above mentioned parameters considered at various iterations. The graphs are sorted based on the maximum displacement values, i.e., the maximum displacement value is sorted from lowest to highest. The extreme left and right sides of the curve in the first graph represent the best and worst solutions respectively. In comparison with the first graph, the corresponding values of height, divisions in the base geometry and point in the upper geometry considered are also sorted based on the fitness value sorting. Here, it can be seen that the best solution refers to the lowest maximum displacement value of 0.114068 cm and the worst solution value is 2.0768 cm.

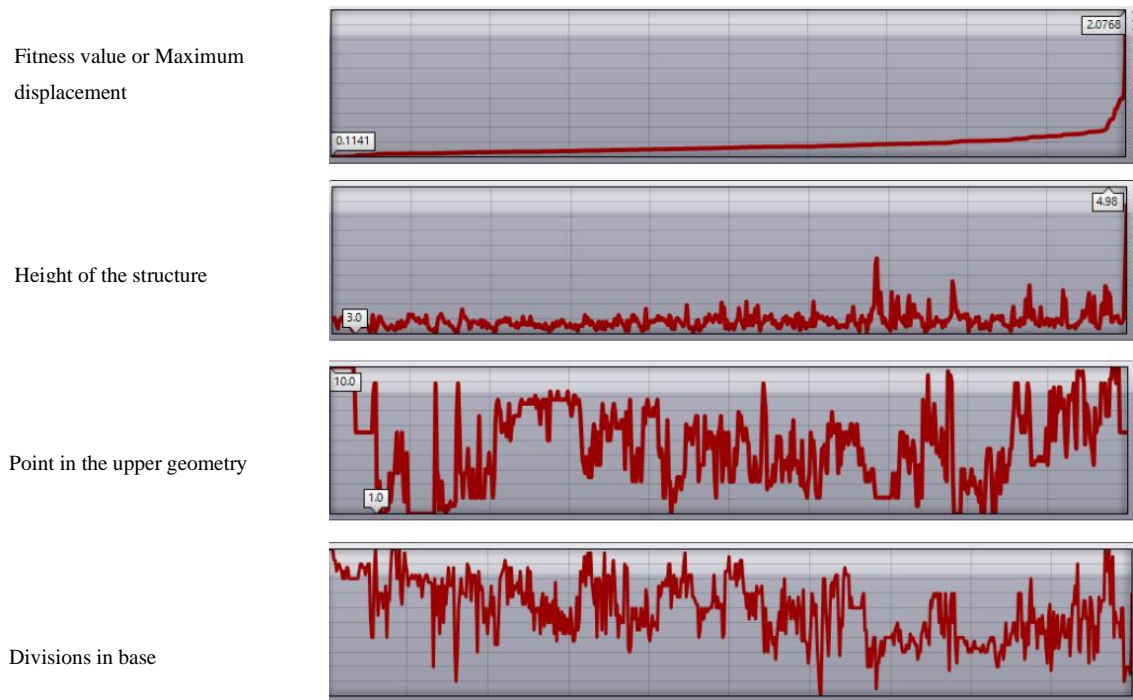


Figure 4.2: Algorithm output graphs for Case 1

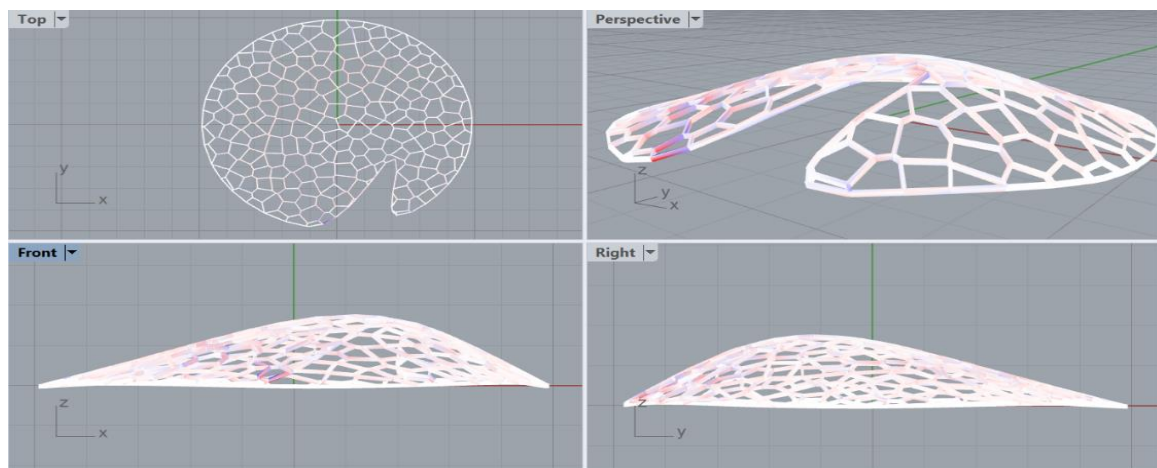


Figure 4.3: Algorithm visual output for Case 1

4.1.2 Case 2: Form with Single Opening and Relaxed Voronoi Tessellation

Aim: To obtain the form of the structure with a single opening, which results in minimum displacements.

Inputs: Table 4.3 defines the various types of parameters with which a shell structure attains a shape. The parameters include the width and height of the base geometry (circular), number of Voronoi panels and its dimensions set between a certain range based on visualization. The single opening of the structure is obtained in a similar way as mentioned in case 1. Genetic algorithm is set to a similar configuration as in case 1, i.e., the number of individuals in each generation is set to 20 with an initial boost of 40 and the maximum number of stagnant generations before the algorithm aborts are set to 50 and fitness value is subjected to minimization.

Table 4.3: Geometrical inputs for Case 2

Preliminary set up	Value	Description
Base Width	10 m	User's choice
Base Length	10 m	User's choice
Voronoi cells	210	User's choice
Lloyd's iteration	160	User's choice
Approximate range for the length of each side of panel	0.2 m to 0.8 m	Depends on number of Voronoi cells and relaxation (visual check)

Table 4.4: Inputs for Genetic algorithm of Case 2 (Galapagos)

Gene Pool	Form	Range set	Type of value	Influence
Height	Number slider	3.00 to 5.00	Real (two decimals)	Structure height
Division in base geometry	Number slider	10 to 20	Integer	Structure shape
Point in upper geometry (point 1)	Number slider	1 to 10	Integer	Structure shape

Outputs: After the execution of the genetic algorithm, the following outputs are obtained defining the lowest fitness value, i.e., maximum displacement has the lowest value of all the generations. The shell structure with the lowest displacement can be seen with colour codes signifying low axial stresses (see Appendix A3).

- Height of the structure = 3.26 m
- Division in base geometry = 11 divisions
- A point in the upper geometry = 9th point
- Fitness value or Maximum displacement = 0.133578 cm
- Number of iterations / combinations checked = 2421

The following graphs represent the values of the above mentioned parameters considered at various iterations. The extreme left and right sides of the curve in the first graph represent the best and worst solutions respectively. Here, it can be seen that the best solution refers to the lowest maximum displacement value of 0.133578cm and the worst solution value is 1.9128cm. The comparison and conclusions with reference case 1 are mentioned in the Conclusions section.

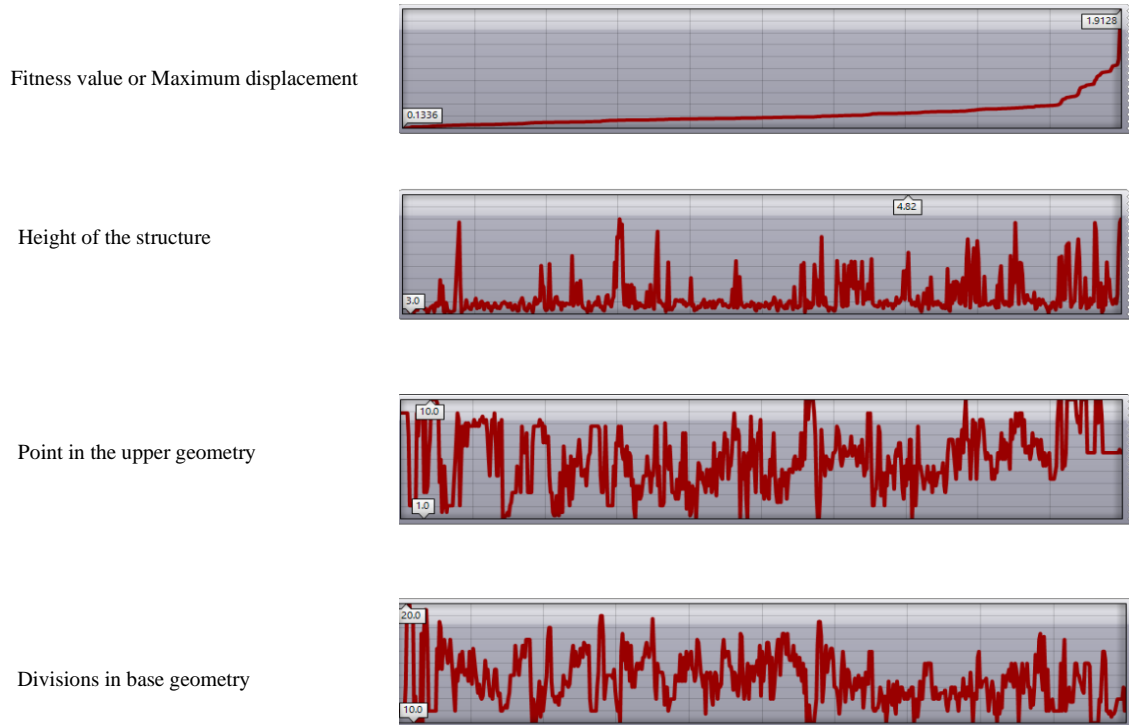


Figure 4.4: Algorithm output graphs for Case 2

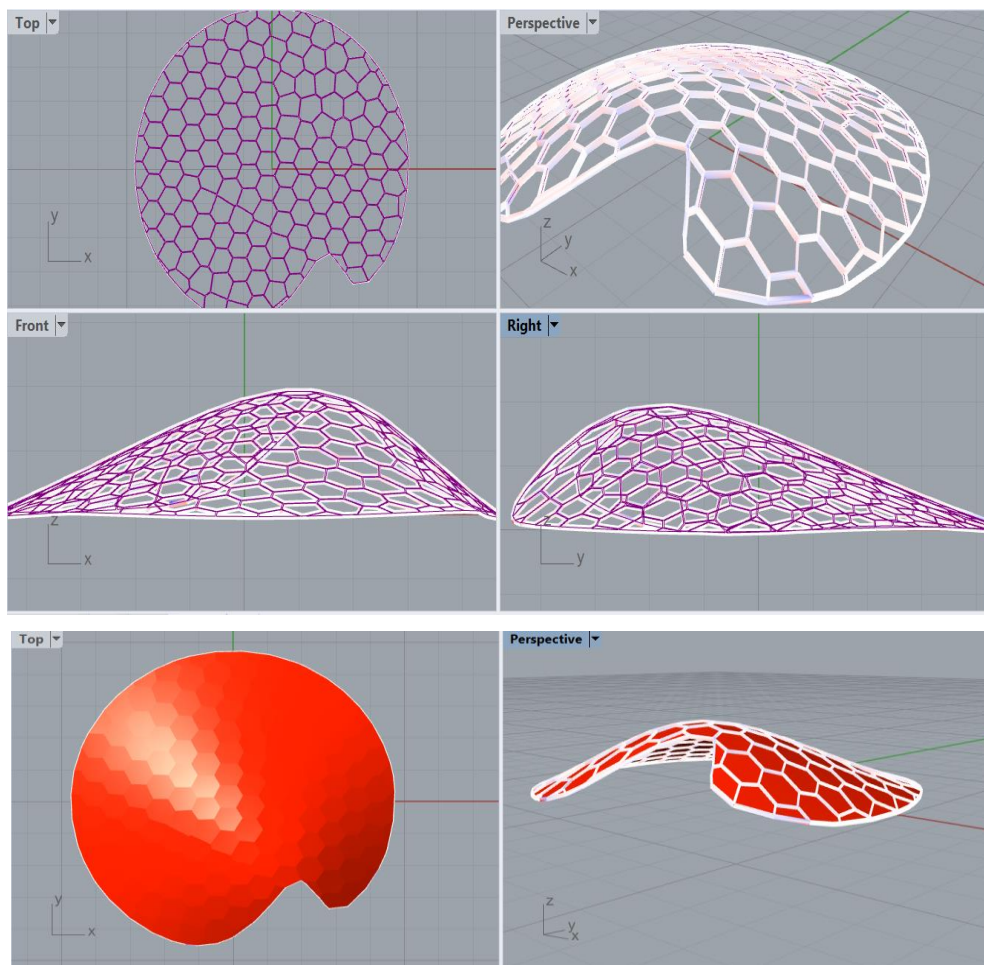


Figure 4.5: Algorithm visual output for Case 2

4.1.3 Case 3: Form with Double Openings and Relaxed Voronoi Tessellation

Aim: To obtain the form of the structure with double openings, which results in minimum displacements.

Inputs: Table 4.5 defines the various types of parameters with which a shell structure attains a shape. The parameters include the width and height of the base geometry (circular), number of Voronoi panels and its dimensions set between a certain range based on visualization. The double opening of the structure is obtained by inserting a point of the upper geometry into the positions 3 and 8 of the NURBS list. Table 4.6 defines the inputs for genetic algorithm and configuration is similar to the other cases, i.e., the number of individuals in each generation is set to 20 with an initial boost of 40 and a maximum number of stagnant generations before the algorithm aborts are set to 50 and fitness value is subjected to minimization.

Table 4.5: Geometrical inputs for Case 3

Preliminary set up	Value	Description
Base Width	10 m	User's choice
Base Length	10 m	User's choice
Voronoi cells	210	User's choice
Lloyd's iteration	160	User's choice
Approximate range for the length of each side of the panel	0.2 m to 0.8 m	Depends on the number of Voronoi cells and relaxation (visual check)

Table 4.6: Inputs for Genetic algorithm of Case 3 (Galapagos)

Gene Pool	Form	Range set	Type of value	Influence
Height	Number slider	3.00 to 5.00	Real (two decimals)	Structure height
Division in base geometry	Number slider	10 to 20	Integer	Structure shape
Two Points in upper geometry (point 2 and 8)	Number slider	1 to 10	Integer	Structure shape

Outputs: After the execution of the genetic algorithm, the following output is obtained defining the lowest fitness value, i.e., maximum displacement has the lowest value of all the generations (see Figure 4.6). The shell structure with the lowest displacement can be seen with colours code signifying low axial stresses(see Figure 4.7 and Appendix A3).

- Height of the structure = 3.45 m
- Division in base geometry = 20 divisions
- A point in the upper geometry = 9th point
- Fitness value or Maximum displacement = 0.218338 cm
- Number of iterations / combinations checked = 2201

The following graphs represent the values of the above-mentioned parameters considered at various iterations. The extreme left and right sides of the curve in the first graph represent the best and worst solutions respectively. Here, it can be seen that the best solution refers to the lowest maximum displacement value of 0.218338 cm and the worst solution value is 0.317103 cm. The corresponding deformations and the colour codes are shown in the seventh part of Appendix A4. It can be noticed that the maximum displacement value is higher when compared to the other cases due to the fact of including two openings in the structure.

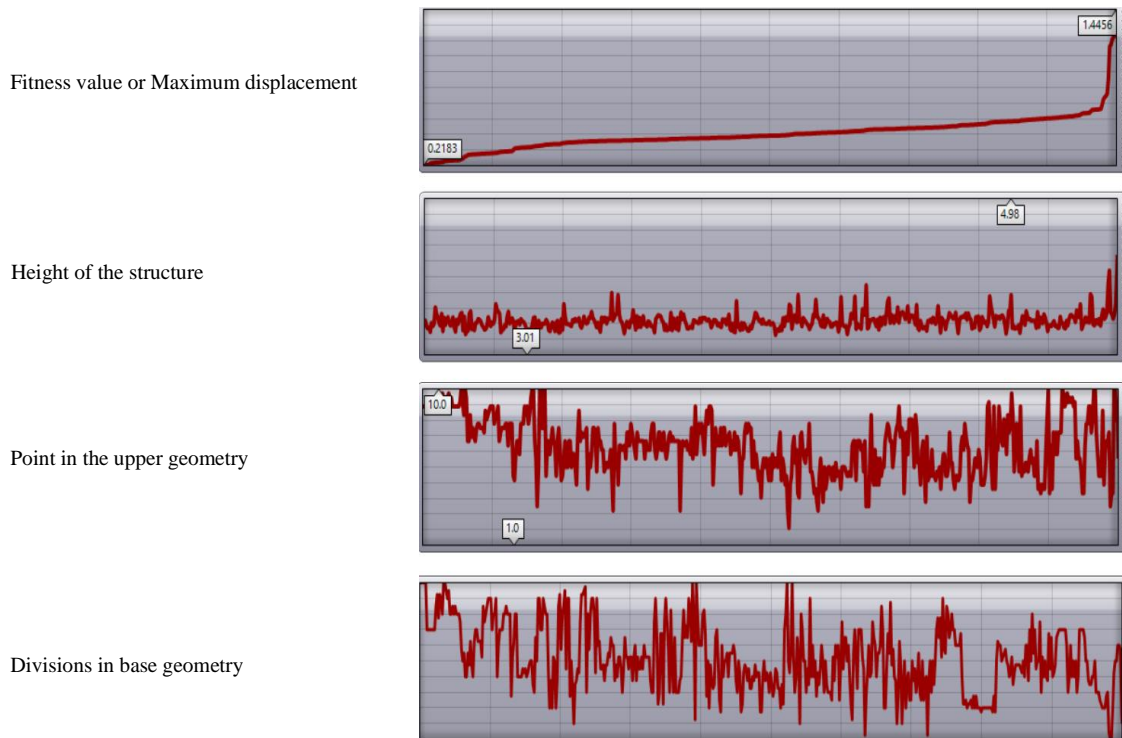


Figure 4.6: Algorithm output graphs for Case 3

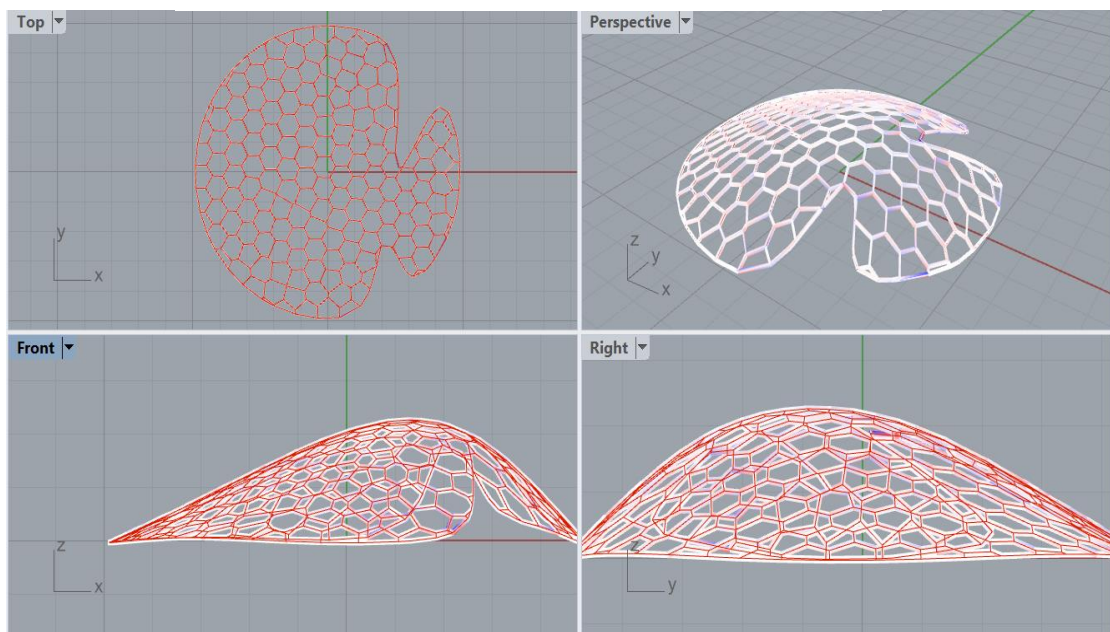


Figure 4.7: Algorithm visual output for Case 3

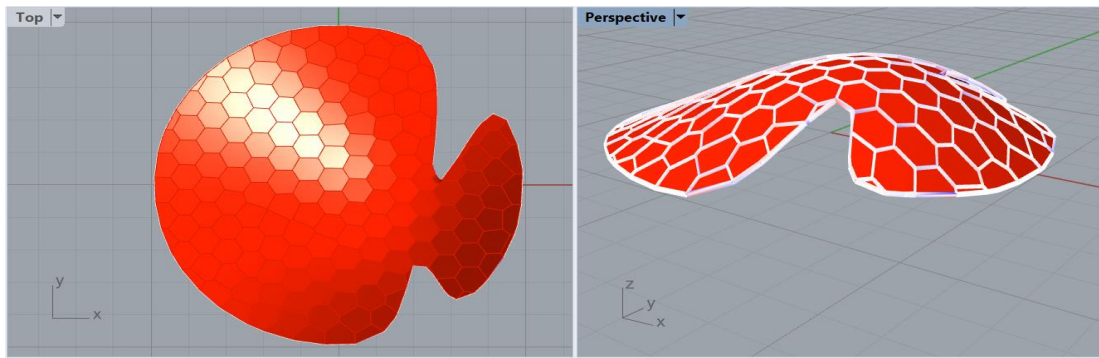


Figure 4.8: Final structure after visualization

4.2 Optimization of Cell or Panel Packing

In this optimization process, the same component Galapagos executes the genetic algorithm for a different purpose, i.e., evenly distributing irregularly shaped geometries representing metal sheet panels on a full-scale metal sheet without collisions. Level of tuning defines how well the panels are packed close to each other.

The optimization process is carried out for six irregularly shaped panels that are obtained by sorting the panels with the area in descending order. The panel extracted after optimization of structure in case 3 (see the previous section) are 28, 46, 49, 158, 166, and 173. The centroids of the panels are used as reference points and transferred to the newly generated points by the two gene pool, i.e., x and y coordinates. The rotation of the panels is also considered to obtain the best fit.

4.2.1 Case 1: Panel Packing for Low Level of Tuning

Inputs: Table 4.7 represents the inputs or the varying parameters fed into the Galapagos component together with population configuration shown in Figure 4.9. The limits for sheet dimensions set are 4.0m in x-direction and 3.0m in the y-direction (hence the values are set between a certain range in Table 4.7). It shall be noted that the dimensions of sheet metal considered is just an assumption and it can vary depending on the availability in the market. This algorithm is universal for any dimensions of the metal sheet.

Table 4.7: Parameters as a gene pool for Galapagos

Gene pool for six panels	Form	Range set	Type of value
x-coordinate	Gene pool	0.0 to 4.0	Real (one decimal)
y-coordinate	Gene pool	0.0 to 3.0	Real (one decimal)
rotation	Gene pool	0.0 to 360.0	Real (one decimal)

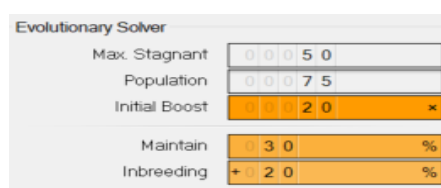


Figure 4.9: Inputs for solver

Table 4.8: Centroidal co-ordinates and rotation angles of panels for initial packing configuration

Panel Number	Co-ordinates	Rotation angle	Sheet Area	Wastage
Panel 28	(1.8, 0.6)	101.3°	9.558 m ²	6.422 m ²
Panel 46	(1.0, 0.1)	113.9°		
Panel 49	(0.8, 2.0)	152.2°		
Panel 158	(2.5, 1.4)	267.7°		
Panel 166	(3.1, 0.1)	194.9°		
Panel 173	(0.4, 1.0)	94.3°		

Table 4.8 represents the gene pools set after randomizing it by 100 percent and it is the initial configuration or panel distribution fed into the Galapagos component (see Figure 4.10). It can be noted that the initial sheet area is 9.558 m² and the material wastage is 6.422 m². The dimensions of metal sheet in x and y direction are 3.51m and 2.723m respectively.

Outputs: After 216 iterations, the genetic algorithm produces a brilliant packing of panels reducing the area approximately near to half of the initial configuration, i.e., the area is 4.523m² and the material wastage is 1.386 m². The corresponding coordinates of panels centroids for the final packing configuration are as shown in Table 4.9 and the final configuration can be seen in Figure 4.11. Also, it can be noticed that the dimensions of the metal sheet in x and y direction are 2.54 m and 1.78 m respectively.

Table 4.9: Centroidal co-ordinates and rotation angles of panels for final packing configuration

Panel Number	Co-ordinates	Rotation angle	Sheet Area	Wastage
Panel 28	(2.8, 2.2)	68.5°	4.523 m ²	1.386 m ²
Panel 46	(2.6, 1.5)	288.6°		
Panel 49	(1.9, 0.4)	164.4°		
Panel 158	(2.8, 0.6)	199.9°		
Panel 166	(1.8, 1.2)	15.7°		
Panel 173	(1.9, 2.1)	21.7°		

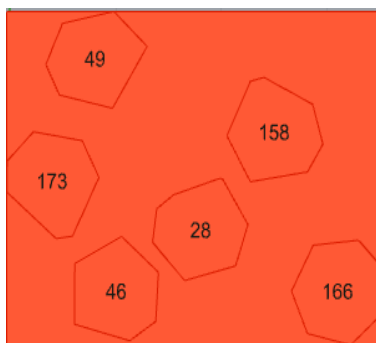


Figure 4.10: Initial packing of panels

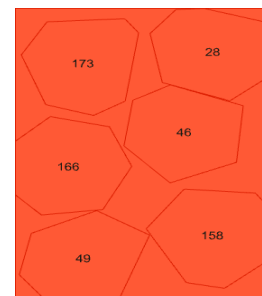


Figure 4.11: Final packing of panels for case 1

4.2.2 Case 2: Panel Packing for High Level of Tuning

Inputs: Table 4.10 represents the inputs or the varying parameters fed into the Galapagos component together with population configuration shown in Figure 4.12. The limits for sheet dimensions set are 4.0m in x-direction and 3.0m in the y-direction (hence the values are set between a certain range in Table 4.10). The major change for fine-tuning is increasing the decimal places of gene pools and change in the range of rotation angle.

Table 4.10: Parameters as a gene pool for Galapagos

Gene pool for six panels	Form	Range set	Type of value
x-coordinate	Gene pool	0.00 to 4.00	Real (two decimals)
y-coordinate	Gene pool	0.00 to 3.00	Real (two decimals)
rotation	Gene pool	-180.000 to +180.000	Real (three decimals)

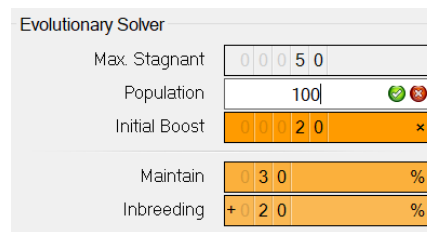


Figure 4.12: Inputs for solver

Table 4.11 represents the gene pools set from the previous case and it is the initial configuration or panel distribution fed into the Galapagos component (see Figure 4.11). It can be noticed that the initial sheet area is 4.523 m² and the material wastage is 1.386 m². The dimensions of metal sheet in x and y direction are 2.54 m and 1.78 m respectively.

Table 4.11: Centroidal co-ordinates and rotation angles of panels for initial packing

Panel Number	Co-ordinates	Rotation angle	Sheet Area	Wastage
Panel 28	(2.8, 2.2)	68.5°	4.523 m ²	1.386 m ²
Panel 46	(2.6, 1.5)	288.6°		
Panel 49	(1.9, 0.4)	164.4°		
Panel 158	(2.8, 0.6)	199.9°		
Panel 166	(1.8, 1.2)	15.7°		
Panel 173	(1.9, 2.1)	21.7°		

Outputs: Figure 4.13 shows the final configuration or panel packing obtained after 956 iterations. It can be noticed that there is a slight drop in the area of sheet metal along with the drop in wastage, i.e., sheet area and wastage have values 4.48477 m² and 1.3487 m² respectively (see Table 4.12). Also, the panel packing is in such a way that the corresponding dimensions of a sheet in the x-direction are lower than the dimension in y directions when compared to the case 1, i.e., values are 1.85 m and 2.42 m respectively.

Table 4.12: Centroidal co-ordinates and rotation angles of panels for final packing

Panel Number	Co-ordinates	Rotation angle	Sheet Area	Wastage
Panel 28	(0.69, 0.82)	-20.678°	4.48477m ²	1.3487 m ²
Panel 46	(2.24, 0.81)	26.368°		
Panel 49	(1.51, 1.04)	-13.563°		
Panel 158	(0.64, 1.65)	24.401°		
Panel 166	(2.22, 1.59)	110.003°		
Panel 173	(1.43, 1.85)	50.173°		

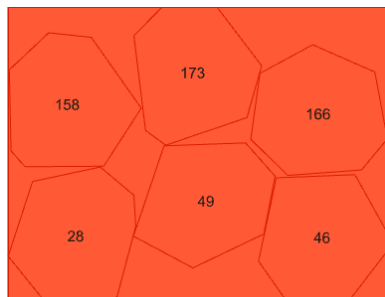


Figure 4.13: Final packing of panels for case 2 (not to scale)

Thus, the optimization attempts for finding structurally stable forms of the shell structure and panel distribution or packing as mentioned above are compared in the next section and conclusions are drawn for these attempts.

5 Conclusions and Future Work

5.1 Conclusions

With reference to the two main objectives of this research work, the study has been carried out based on the concepts available prehistorically and applying those in the currently available evolutionary solvers. The ideas behind the development of shell structures by notable and renowned figures in the engineering world such as Antoni Gaud, Frei Otto and many others along with their achievements was understood. The availability of free form designs and patterns in nature have also been an influence on the development of this optimization algorithm. In addition, the two case studies as real standing structures in two different continents were of great inspiration for this research work.

I. As mentioned in the previous chapters, the first objective of the research work is “Optimization of freeform metal sheet assembled shell structure with respect to structural stability.” As per the requirements of the research work, there was a need for relaxed Voronoi tessellation in the shell structure which directly governs its structural stability based on the form attained by other influencing parameters such as the height of the structure, number of divisions in the base geometry and points in the upper geometry (i.e., number of openings). The research work was carried out by considering a circular base geometry inside a square with 10 m in width and 10 m in length. The results are generated based on the value of the maximum displacement which acts as a fitness value for the genetic algorithm. The following optimized shell structures were achieved by using a genetic algorithm technique;

- **Case 1: Form with Single Opening and Irregular Voronoi Tessellation**

This case acts as a reference case, where there was no relaxation of Voronoi pattern and the resulting stable structure by the genetic algorithm gives the maximum displacement value has as 0.114068 cm. This value has been obtained after the genetic algorithm has performed 2561 iterations with various combination of three different parameters (as mentioned above) included as number sliders in the algorithm. The corresponding values for the other parameters are discussed in the Results and Discussion section.

- **Case 2: Form with Single Opening and relaxed Voronoi Tessellation**

In comparison with the reference case, the relaxation technique was carried out by Lloyd’s algorithm, using a component hoopsnake in Grasshopper. Thus, it can be noticed that the Voronoi tessellations are proportional and well-shaped compared to the reference case. However, the genetic algorithm has resulted in a maximum displacement value of 0.133578 cm for a structurally stable shell structure after 2421 iterations with various combination of three different parameters. The corresponding value of the height of the structure is 3.26 m, which is close to 3.21m in the reference case.. Thus, it can be concluded that there was a greater influence of the Voronoi pattern together with the shape of the surface on the

maximum displacement value. Hence, the resultant value although being greater than the reference case but the genetic algorithm gives aesthetically and structurally acceptable structure with better panel shapes and rounded opening compared to the reference case with irregular panel shapes and sharp cut opening.

- **Case 3: Form with Double Openings and relaxed Voronoi Tessellation**

This case varies from the other two cases because it has two openings compared to the single opening in first and second cases and relaxed Voronoi pattern compared to the first case. The lowest value for maximum displacement is 0.218338 cm after 2201 iterations. The structurally stable form of the shell structure now has 3.45 m as height. It is a well-known fact that when the structure has two openings, the resultant displacements will be higher and hence the value of maximum displacement, in this case, is higher in comparison with the other two cases.

Thus, it can be concluded that the manual approaches to explore a wide variety of forms for being structurally stable and aesthetically pleasing is a time-consuming approach. There are greater risks of inaccurate results and hence the optimization technique using genetic algorithm gives a broader range of designs of the shell structure for the architects that fall under well stable forms according to the regulations. This algorithm helps architects to achieve stable structures by performing basic structural analysis. The detailed structural analysis could be performed by the experts in the field and it can be further used in the algorithm.

II. The second objective of this research study is the “Optimization of cell or panel distribution in full-scale sheet metal for an effective manufacturing process.” The manufacturing techniques as mentioned in section 2.5 gives a brief idea on metal sheet façade manufacturing. However, the panel packing is performed at low-level detail, i.e., Only panel geometry is considered. Details about the bending planes and final cut geometry are neglected due to limited scope of work. To demonstrate the application of genetic algorithm on panel packing, two cases were considered as mentioned below:

- **Case 1: Panel Packing for Low Level of Tuning**

The initial packing configuration was considered after the gene pool consisting of points was randomized by 100 percent. The corresponding sheet area and material wastage for this packing is 9.558 m² and 6.422 m² respectively. After performing the optimization process using the genetic algorithm, the panels were packed close to each other resulting in a sheet area 4.523 m² and wastage 1.386 m² after 216 iterations. Thus, it can be noticed that there was considerable and successful packing of panels carried out by the genetic algorithm. However, there were minor gaps and the edges of the panel geometry were not close to each other as desired due to the fact of defining the lower number of decimal places for the points

to move and rotate. Therefore, another attempt was carried out and is as mentioned in the flowing case.

- **Case 2: Panel Packing for High Level of Tuning**

In this case, the initial packing configuration considered is the packing configuration obtained in case 1. In this case, the gene pool was modified by placing three decimal places values and the rotation angle range between -180° to $+180^\circ$. After execution of the genetic algorithm, the resulting sheet area was noticed to have impacted a minor change on the sheet area and wastage value after 956 iterations. But the orientation and placements of panels close to each other were observed to have incredible changes and were as desired. The values obtained for sheet area and wastage were 4.48477 m^2 and 1.3487 m^2 respectively.

Thus, it can be concluded that the above-mentioned attempts for panel packing were successful and further tuning can be performed to achieve better results. However, an increasing number of genes to come up with the perfect packing takes higher computation time and it is not feasible for this type of application having higher computation time and produce a slightly better result than the ones obtained above. Hence, only two cases were performed to show the impact of the initial point distribution, orientation and increased gene pool on the final results of panel packing.

5.2 Future work

In this research work, there were two main objectives namely (i) Optimization of freeform metal sheet assembled shell structure with respect to structural stability and (ii) Optimization of cell or panel distribution in full-scale sheet metal for an effective manufacturing process. For former, the optimization process was carried for a low level of structural analysis and the latter, the cell or panel packing was carried for the geometrical shape of the panels. This research work can be extended in various aspects as mentioned below:

1. With reference to the former optimization process, the research shall be carried out for developing complete flat panels. The achievement of complete panels in the shell structure shall be in accordance with the agent-based modelling technique as learned from the case study - The BUGA Wood pavilion.
2. Once the flat panels are achieved, the detailed structural analysis shall be performed in accordance with the EURO Codes and achieve a fitness value that governs a particular model.
3. Since in this research work, the panels generated are near to flat and has deviations and further, the packing process for these panels was attained by projecting on to the local planes. If these panels are produced flat, those flat panels can be used for packing algorithm.
4. The flat panels shall be packed with a high level of details as mentioned below-
 - The bending angle between any two panels based on the curvature of the shell structure shall be considered.
 - This bending angle shall be used to define the corner cuts of the panel.
 - This bending shall be used to define the offset in the geometry for final cutting designs in sheet metal.
5. Exploration of more shell structure designs and other optimization techniques shall be carried out and compared.
6. Study on the influence of different tessellation shaped panels shall be compared with the Voronoi tessellation shell structure.

Bibliography

- [1] R. Naboni, “Form-finding to fabrication of super-thin anisotropic gridshell Form-finding to fabrication of super-thin anisotropic gridshell,” no. November, 2016.
- [2] M. Dimčić, “Structural Optimization of Grid Shells,” Universität Stuttgart, 2011.
- [3] M. VELTKAMP, “Free Form Structural Design, Schemes, Systems & Prototypes of Structures for Irregular Shaped Buildings,” 2007.
- [4] W. J. Lewis, “Computational form-finding methods for fabric structures,” no. January 2008, 2017.
- [5] S. Huerta, “Structural Design in the Work of Gaudi,” vol. 49, no. Tarragó 1991, pp. 324–339, 2006.
- [6] K.-E. Kurrer, *Geschichte der Baustatik*. Berlin: Ernst & Sohn, 2002.
- [7] C. Lang, “NYC-Architecture. (New York Architecture),” 2004. [Online]. Available: <http://www.nyc-architecture.com/BKN/BKN002.htm>. [Accessed: 18-Mar-2020].
- [8] Reinhardcwieland, “Sydney Opera House, Australia,” 2017. [Online]. Available: <https://pixabay.com/photos/sydney-opera-australia-2910646/>. [Accessed: 18-Mar-2020].
- [9] L. Piegl and W. Tiller, *The NURBS Book*. Springer Verlag, 1995.
- [10] W. Pokojski and P. Pokojska, “Voronoi diagrams – inventor , method , applications,” no. December, 2018.
- [11] J. Boissonnat and M. Yvinec, *Curved Voronoi Diagrams*, no. June 2014. 2007.
- [12] Q. Du, M. Emelianenko, and L. Ju, “Convergence of the Lloyd Algorithm for Computing Centroidal Voronoi Tessellations,” no. December 2013, 2006.
- [13] V. Fabert and M. Gunzburger, “Centroidal Voronoi Tessellations : Applications and Algorithms Author (s): Qiang Du , Vance Faber and Max Gunzburger Published by : Society for Industrial and Applied Mathematics Stable,” vol. 41, no. 4, pp. 637–676, 2020.
- [14] “Fractory-Metal sheet Manufacturing,” 2020. [Online]. Available: <https://fractory.com/sheet-metal-bending/>. [Accessed: 22-Mar-2020].
- [15] C. Darwin, *On The Origin Of Species*. Dover Publications, 2006.

- [16] A. E. Eiben and J. E. Smith, *Introduction to evolutionary computing*, Vol. 53. H. 2003.
- [17] A. Gad, “Introduction to Optimization with Genetic Algorithm,” 2018. [Online]. Available: <https://towardsdatascience.com/introduction-to-optimization-with-genetic-algorithm-2f5001d9964b>. [Accessed: 18-Mar-2020].
- [18] H. J. Wagner, O. D. Krieg, O. Kyjanek, and D. Sonntag, “The Buga Wood Pavilion,” no. October, 2019.
- [19] A. Menges and J. Knippers, “BUGA Wood Pavilion 2019,” 2019. [Online]. Available: <https://www.icd.uni-stuttgart.de/projects/buga-wood-pavilion-2019/>. [Accessed: 19-Mar-2020].
- [20] S. Bechert, A. Groenewolt, O. D. Krieg, and A. Menges, “Structural Performance of Construction Systems for Segmented Timber Shell Structures,” *Int. Assoc. Shell Spat. Struct.*
- [21] A. Pena, “Rationalisation of freeform façades : A technique for uniform hexagonal panelling,” no. February, 2014.
- [22] R. Naboni, P. Milano, and R. Naboni, “Form-finding to fabrication of super-thin anisotropic gridshell Form-finding to fabrication of super-thin anisotropic gridshell,” no. November, 2016.
- [23] M. Mosoarca, A. Anastasiadis, and A. Kampouris, “Are Free Form Architecture Ecological Buildings ?,” vol. 373, no. 1, pp. 366–373, 2014.
- [24] R. Bharat, “Leaf,” 2019. [Online]. Available: <https://www.flickr.com/photos/12x/1064398625/sizes/z/in/photostream/>. [Accessed: 19-Mar-2020].
- [25] J. Ito, “Dragonfly wings,” 2007. [Online]. Available: <https://www.flickr.com/photos/35034362831@N01/698898343/>. [Accessed: 19-Mar-2020].
- [26] “Soumaya Museum / FR-EE Fernando Romero Enterprise,” 2011. [Online]. Available: <https://www.archdaily.com/452226/museo-soumaya-fr-ee-fernando-romero-enterprise>. [Accessed: 19-Mar-2020].
- [27] F. Romero and A. Ramos, “Museo Soumaya,” *FREE, Museo Soumaya, Mexico City*,

Mexico, 2011.

- [28] “Museo Soumaya - Mexico City, Mexico,” 2014. [Online]. Available: <https://researchreferences.files.wordpress.com/2014/09/soumayga.jpg>. [Accessed: 19-Mar-2020].

Appendix

A1: Support position, reaction forces and moments for double opening relaxed Voronoi tessellation (Case 3)

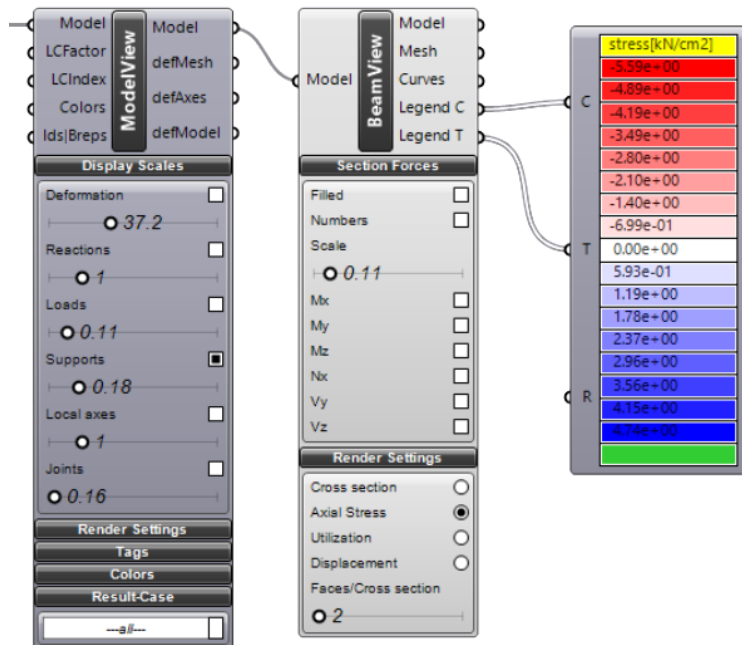
Nr.	Support position	Reaction Forces	Reaction Moments
0	{-4.509269,- 0.572066,0.117618}	{3.146985,0.854694,2.991618}	{-0.003665,-0.737604,-0.083607}
1	{-1.308381,4.732029,-0.000498}	{0,0,0.128429}	{-0.001041,0.00296,0}
2	{-1.234747,4.750467,-0.003112}	{-0.9295,-4.257187,2.513746}	{-0.469823,-0.085339,-0.121784}
3	{-1.930198,4.51425,0.02666}	{2.72705,-2.422403,2.317745}	{-0.321297,-0.374241,-0.113074}
4	{-2.476541,-4.239154,0.066016}	{0,0,0.128047}	{0.002251,0.002804,0}
5	{-3.162023,-3.755801,0.065199}	{3.319097,3.550377,3.24563}	{0.277965,-0.3061,0.089876}
6	{-2.445058,-4.224135,0.080565}	{0.641024,4.829664,3.052554}	{0.292286,-0.073955,0.035049}
7	{-3.912887,-2.553456,0.127504}	{3.747419,1.725125,3.298257}	{0.422614,-0.591013,0.007681}
8	{4.493087,1.97921,0.142092}	{0.68255,-1.133791,2.571604}	{-0.196657,0.933698,-0.090751}
9	{4.757496,1.21235,0.055587}	{-2.71573,-2.01574,3.437436}	{0.101704,0.455766,0.185887}
10	{4.385734,-2.206628,0.148198}	{-5.24845,2.419427,8.295004}	{-0.54824,0.631324,0.055224}
11	{-1.238592,-4.750814,0.028575}	{0,0,0.284248}	{0.001288,-0.000267,0}
12	{-2.026378,-4.471898,0.056173}	{4.757426,2.750191,2.788081}	{0.089604,-0.092305,0.016908}
13	{-1.24043,-4.590065,0.133489}	{-2.947528,5.46017,3.249713}	{0.154073,-0.136727,0.111631}
14	{-4.808352,0.961196,-0.015713}	{0,0,0.168648}	{-0.002285,-0.001873,0}
15	{-4.684462,1.469598,-0.000262}	{0,0,0.122906}	{-0.001542,0.000336,0}
16	{-4.606449,1.698586,0.008385}	{0,0,0.087941}	{0.002482,-0.001582,0}
17	{-4.441004,1.696651,0.068944}	{1.82424,-2.894203,1.560737}	{-0.260349,-0.333075,0.023473}
18	{-4.464361,0.957582,0.121788}	{3.364171,0.488182,3.05056}	{-0.155935,-0.731718,-0.024505}
19	{-4.456182,-2.061005,0.000786}	{0,0,0.186276}	{0.003368,-0.00096,0}
20	{-4.709249,-1.359218,-0.020213}	{0,0,0.22209}	{0.000816,-0.001019,0}
21	{-4.525008,-1.358989,0.056332}	{2.093749,2.797985,1.599461}	{0.24593,-0.289936,-0.042566}
22	{-4.253359,-1.753511,0.124079}	{3.556479,0.75922,3.361035}	{0.077379,-0.883185,0.13842}
23	{-0.492952,4.872781,-0.024422}	{-0.79125,-4.62136,2.758718}	{-0.351555,-0.09004,-0.185754}
24	{0.303141,4.886004,-0.0264}	{0,0,0.247962}	{-0.00237,0.000121,0}
25	{0.31358,4.565111,0.146361}	{-3.82356,-0.30998,5.397719}	{-1.117296,0.15885,0.192287}
26	{-2.066772,-4.453361,0.057326}	{0,0,0.11012}	{0.002205,0.003826,0}
27	{-2.280529,4.347903,0.040071}	{0,0,0.11364}	{0.00032,-0.000783,0}
28	{-2.358603,4.280895,0.051593}	{0.37066,-3.981603,2.386145}	{-0.632283,-0.229294,-0.095118}

29	{4.566558,-1.546075,0.129988}	{-5.34739,2.877396,5.410685}	{-0.020906,-0.144483,-0.002087}
30	{-3.697423,-3.22997,0.049727}	{2.620808,3.693713,2.843382}	{0.334332,-0.24874,-0.065073}
31	{-4.862413,-0.569591,-0.03309}	{0,0,0.257549}	{-0.00027,-0.002718,0}
32	{-4.178978,-2.577037,0.022732}	{0,0,0.229032}	{-0.001566,-0.002789,0}
33	{-3.767226,2.866465,0.113669}	{2.02420,-2.962047,2.736972}	{-0.651413,-0.548157,0.022312}
34	{-3.519379,3.32572,0.082369}	{3.45660,-0.360047,1.880745}	{-0.146087,-0.532192,-0.052127}
35	{0.409245,-4.885807,0.062964}	{-3.20591,8.177826,9.084786}	{0.772167,-1.076219,0.485461}
36	{-0.410432,-4.89242,0.014492}	{-1.538911,4.970172,4.15512}	{0.081706,-0.236557,0.288727}
37	{1.080444,4.784836,0.002839}	{0,0,0.078855}	{0.000575,0.004444,0}
38	{1.12927,4.77061,0.00789}	{0.718837,-1.463799,0.65791}	{-0.302079,-0.407886,-0.288031}
39	{1.122694,4.61292,0.094683}	{-11.32101,10.04242,10.4715}	{-2.061493,-1.317616,-0.613469}
40	{-2.999375,3.886813,0.05803}	{1.066166,-3.163659,2.10578}	{-0.447965,-0.27539,-0.031944}
41	{-2.386863,4.290451,0.043667}	{0,0,0.211142}	{-0.002121,0.003182,0}
42	{4.861684,0.684568,-0.000021}	{0,0,0.246064}	{0.001089,0.00035,0}
43	{4.884633,0.315492,-0.015303}	{-3.55065,-0.80548,4.201319}	{0.101869,0.178223,0.074676}
44	{4.660385,-1.544412,0.035956}	{0,0,0.178476}	{-0.002849,0.001442,0}
45	{-4.486728,0.200918,0.139328}	{3.300963,0.989206,2.889629}	{-0.036278,-0.827929,-0.057544}
46	{-4.338013,2.299133,0.030862}	{0,0,0.202806}	{-0.00061,-0.000838,0}
47	{-3.980736,2.873595,0.049134}	{0,0,0.147365}	{-0.000418,-0.00096,0}
48	{-4.224983,2.123198,0.093434}	{3.55054,-0.100341,2.596812}	{-0.142938,-0.763298,-0.002128}
49	{4.847615,-0.623106,-0.021494}	{-5.54898,0.190733,5.816747}	{0.019768,-0.13743,-0.018649}
50	{-4.892212,0.204828,-0.031437}	{0,0,0.504269}	{-0.000204,-0.003248,0}
51	{-3.559754,3.381303,0.058798}	{0,0,0.169899}	{0.000282,-0.001106,0}
52	{4.748217,-1.248811,-2.5365e-6}	{0,0,0.168319}	{0.002231,-0.000262,0}

A2: Normal forces, shear forces and bending moments for all elements for double opening relaxed Voronoi tessellation

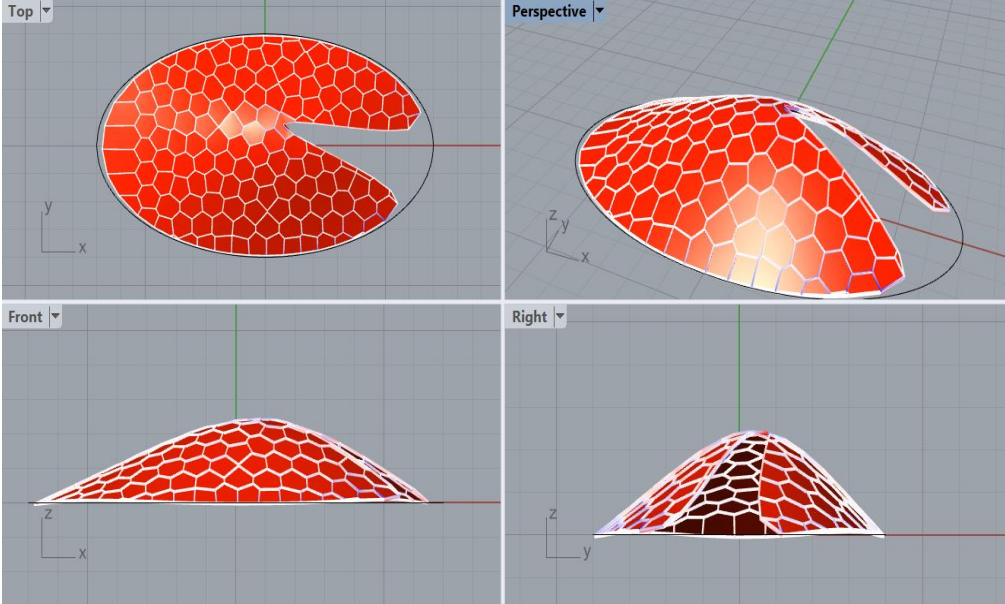


A3: Grasshopper components for stresses and deformation visualization in Rhino for double opening relaxed Voronoi tessellation

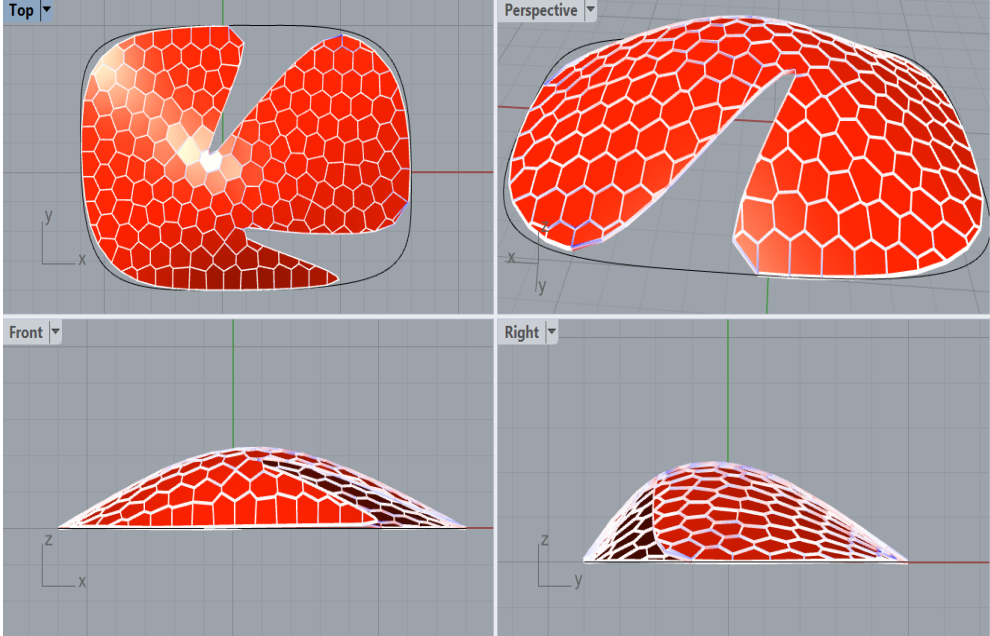


A4: Some examples of variations in base geometry

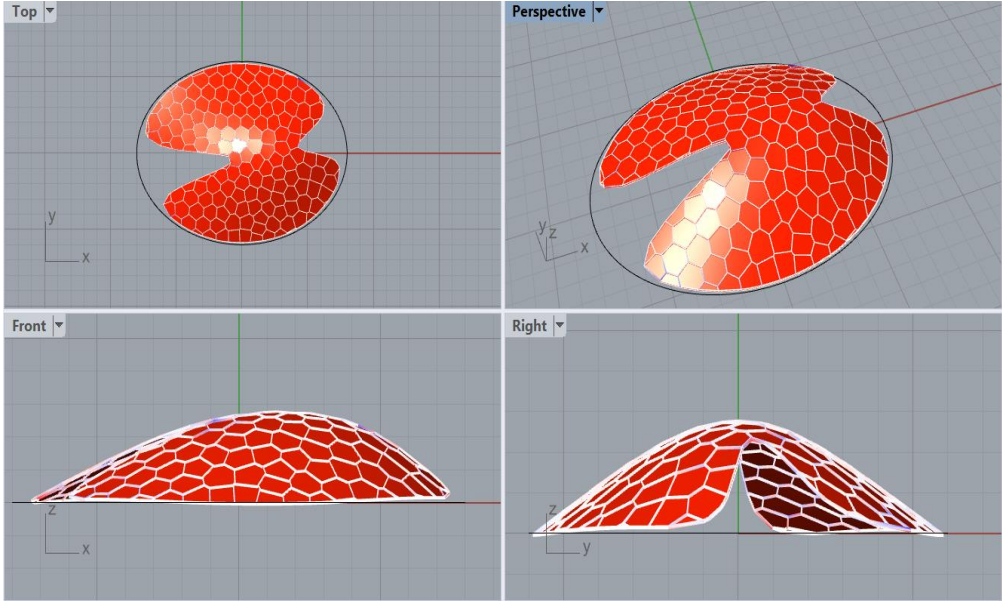
1. Ellipse as a base geometry with a single opening



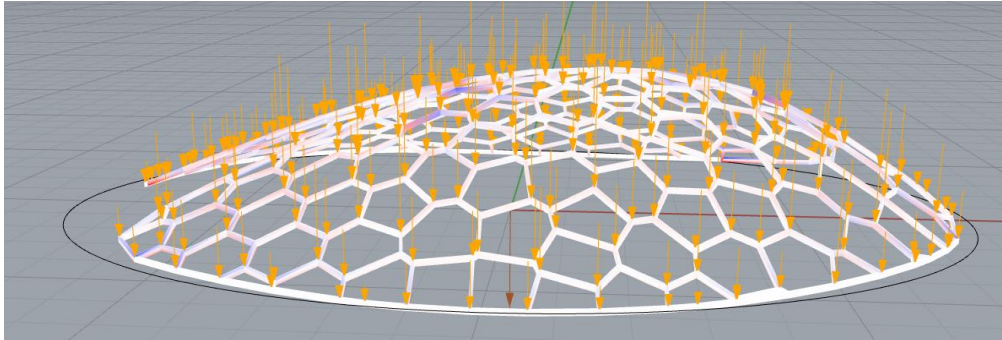
2. Freeform base geometry with double opening



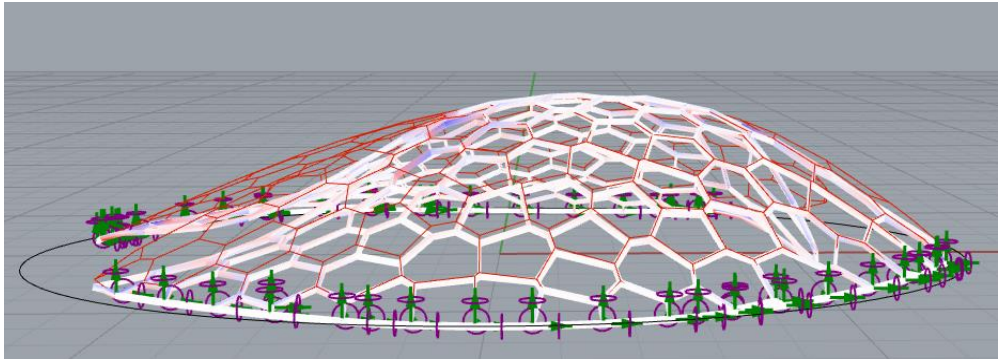
3. Ellipse as a base geometry with double openings



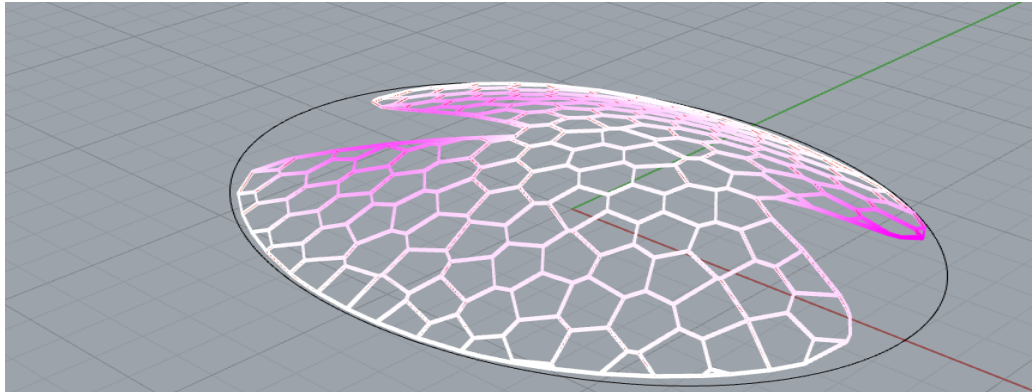
4. Ellipse as a base geometry with double openings and applied loads



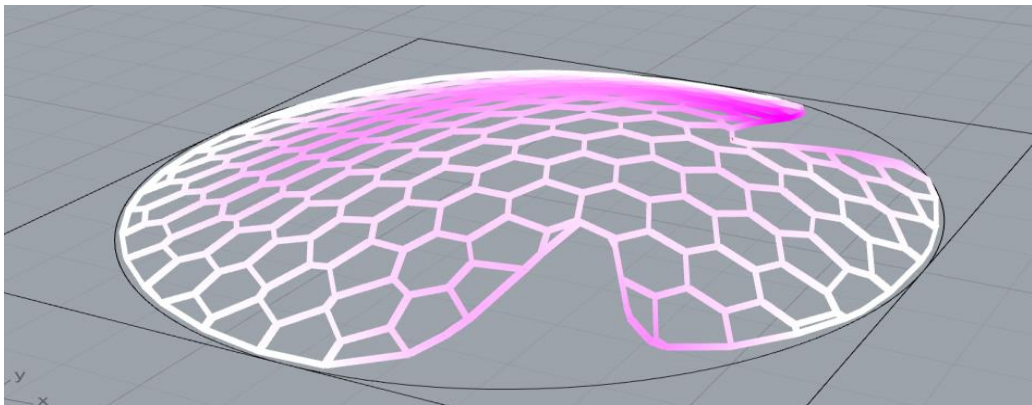
5. Deformation in elements of the structure formed by ellipse as a base geometry (double openings)



6. Deformation of the structure formed by ellipse as a base geometry (double openings)



7. Deformation of the structure formed by a circle as a base geometry (for Case 3 having double openings)



8. Reaction forces at supports for the structure formed by a circle as a base geometry (For Case 3 having double openings)

